Primary and secondary signals of variations in the Denmark Strait Overflow over the last glacial cycle

Kumulative Dissertation
zur Erlangung des Doktorgrades
der Mathematisch-Naturwissenschaftlichen Fakultät
der Christian-Albrechts-Universität
zu Kiel

vorgelegt von
Christian Millo

Kiel, 2005

Abstract

The Denmark Strait Overflow (DSO) today carries cold (-1°C) and dense bottom water into the Northern North Atlantic, and in part counterbalances the northward inflow of warm surface water of the North Atlantic Current and its ramifications. This heat and mass balance profoundly influence the modern Atlantic thermohaline circulation. A quantitative reconstruction of the intensity of overturning rates during past ocean scenarios such as the Last Glacial Maximum (LGM) is a fundamental but yet open objective of paleoceanography.

In the first part of this study, we reconstruct the variability of the DSO for the LGM up to the transition to Heinrich meltwater event I on the basis of four new and several published planktic and epibenthic stable isotope records obtained from sites to the north and south of the Denmark Strait. The spatial and temporal pattern of epibenthic $\partial^{18}O$ and $\partial^{13}C$ maxima across the LGM Denmark Strait reveal a north-south density gradient from σ_0 ~ 28.7 to 28.1 at 800 – 1800 m water depth and suggest ongoing convection of dense and highly ventilated water in the Nordic Seas and a glacial DSO that was directed to the south like today, eventually forming the glacial North Atlantic Deepwater. To the south of Iceland a further convection cell of Glacial North Atlantic Intermediate Water is documented by less high density (σ_0 ~ 28.1) but extremely high epibenthic $\partial^{13}C$ values (~ 1.70‰) that implies a strong ventilation on top of the Mid Atlantic Ridge.

In Chapter 3 we present striking planktic and epibenthic $\partial^{13}C$ values reaching up to –7‰, as documented in two coeval sediment records obtained from the southeastern Greenland margin and the adjacent basin floor over Marine Isotope Stage (MIS) 5.2 - MIS 5.1 and over stadial-to-interstadial times in MIS 4 and early MIS 3. ^{13}C-depleted foraminifera possibly integrated a primary (down to –2.5‰) and a post-depositional (~ -20‰) light $\partial^{13}C$ signatures resulting from thermal instability of (strongly ^{12}C-enriched) methane hydrates and subsequent oxidation of methane in pore and ocean water. Methane hydrates possibly dissociated during short-term inversions of the DSO and inherent incursions of relatively warm (up to ~ 8°C) Upper Atlantic Intermediate Water into the Greenland Sea basin, events that resulted from a short-term meltwater-induced shut-off of deepwater formation in the Nordic Seas.

Kurzfassung

Der Denmark Strait Overflow (DSO) transportiert heute kaltes (-1°C), dichtes Bodenwasser in den nördlichen Nordatlantik, wodurch der nordwärts gerichtete Einstrom der warmen Oberflächenwassermassen des Nordatlantikstroms teilweise ausgeglichen wird. Dieses Massen- und Wärmegleichgewicht beeinflusst die atlantische thermohaline Zirkulation tiefgreifend. Eine quantitative Rekonstruktion der Intensität der „overturning"-Raten vergangener Szenarien wie des Letzten Glazialen Maximums (LGM), ist deshalb eine grundsätzliche, noch offene Frage der Paläoozeanographie.

Im ersten Teil dieser Arbeit wird die Variabilität des DSO während des LGM bis zum Schmelzwasserereignis Heinrich I rekonstruiert, auf Grundlage vier neuer, sowie mehrerer publizierter Zeitserien stabiler Isotope planktonischer und epibenthischer Foraminiferen, von Kernpositionen nördlich und südlich der Dänemark Straße. Das räumliche und zeitliche Muster der epibenthischen $\partial^{18}O$ und $\partial^{13}C$ Maxima entlang der Dänemark Straße zeigt im LGM einen Nord-Süd-Dichte-Gradienten von σ_0 ~ 28,7 bis 28,1 in Wassertiefen von 800 – 1800 m. Dies weist auf fortlaufende Konvektion von dichten, gut durchlüfteten Wassermassen im Nordmeer mit einer wie heute südwärts gerichteten Ablenkung des DSO, der schließlich zur Bildung von glaziale nordatlantische Tiefenwassers beiträgt. Südlich von Island belegen extrem hohe epibenthische $\partial^{13}C$ Werte (~ 1,70‰) zusammen mit einer ebenfalls hohen Dichte (σ_0 ~ 28,1) eine weitere Konvektionszelle glazialen nordatlantischen Zwischenwassers, indem sie eine gute Belüftung des Wassers über dem Mittelatlantischen Rückens bezeugen.

In Kapitel 3 werden ungewöhnlich leichte (bis zu -7‰) planktische und epibenthische $\partial^{13}C$ Werte aus zwei Sedimentkernen vom südöstlichen grönländischen Kontinentalhang und angrenzendem Becken vorgestellt. Diese traten jeweils in den marinen Isotopenstadien (MIS) 5.2 – 5.1 sowie in den Stadial-Interstadialen im Übergang von MIS 4 zum frühen MIS 3 auf. Diese ^{13}C abgereicherten Foraminiferen integrierten möglicherweise primäre (bis zu -2,5‰) und sekundäre (post-depositionale ~ -20‰) extrem leichte ^{13}C Signaturen, die aus thermisch instabil gewordenen (stark an ^{12}C angereicherten) Methanhydraten, und anschließender Oxidation des Methans im Poren- und Meerwasser stammen. Methanhydrate dissoziierten möglicherweise während kurzfristiger Ereignisse einer Umkehr des DSO, verbunden mit dem Einstrom von relativ warmem (bis zu ~ 8°C) oberen atlantischen Zwischenwasser in das Becken der Grönlandsee, gesteuert durch einen Schmelzwasser-induzierten Zusammenbruch der Tiefenwasserbildung im Nordmeer.

Contents

CHAPTER 1
Introduction

1.1 Background

The Denmark Strait Overflow (DSO) today forms a giant cataract which carries cold and dense water from the Greenland Sea into the Northern North Atlantic. This current is a major component (3 x 10^6 m^3/s = 3 Sv) of the total southward outflow of deepwater (6 Sv) from the Nordic Seas into the Atlantic Ocean. An additional flux of low salinity and low density surface water reaches the North Atlantic through the Canadian Archipelago (1.7 Sv) and via the East Greenland Current (EGC) (1.3 Sv). This southward outflow of cold water compensates for the inflow (8 Sv) of warm and saline surface water of Atlantic origin into the Greenland-Iceland-Norwegian Seas (1 Sv from the Pacific Ocean reaches the Arctic Ocean through the Bering Strait) (Hansen & Østerhus, 2000). This mass balance is a key factor governing the modern Atlantic Thermohaline Circulation (THC) system and thus the poleward heat transport in the northern hemisphere.

The strength of the DSO mainly depends on the density contrast between the water masses to the north and south of the Denmark Strait (Whitehead et al., 1974), and therefore is particularly sensitive to changes in sea surface salinity due to meltwater release from the neighbour ice sheets (Hansen et al., 2001; Dickson et al., 2002). Significant changes in the intensity and direction of the DSO are expected to have occurred on geological time scales owing to perturbations of the density pattern during episodes of major freshwater discharge into the Nordic Seas, such as during the Dansgaard-Oeschger (DO) stadials and Heinrich Events (H). For example, meltwater pulses, inferred from light planktic $\partial^{18}O$ anomalies in the Nordic Seas, led to a cessation of deepwater formation documented by a dramatic reduction in benthic $\partial^{13}C$ values during the H1 (15 kyrs BP) (Sarnthein et al., 2000). The weakening or complete shut off of surface ocean convection caused an inversion of North Atlantic THC and possibly led to a DSO reversal which resulted in a northward incursion of relatively warm and highly saline Atlantic Upper Intermediate Water into the Nordic Sea during major Dansgaard-Oeschger stadials (Rasmussen & Thomsen, 2004).

Significant changes in the DSO regime are also expected for the Last Glacial Maximum (LGM). In this period, ice sheets constricted the Denmark Strait aperture from both sides (Larsen, 1983). Moreover the eustatic sea level reduction by 120 to

130 m (Lambeck & Chapell, 2001) and glacio-eustatic rebounds induced by changes in the volume of continental ice sheets on Greenland and Iceland (Fleming & Lambeck, 2004) diminished the maximum depth of the Denmark Strait sill by about 130 m (today 630 m) and possibly reduced the intensity of DSO.

Model simulations of the DSO over the LGM suggest a substantial decrease of its flux to 0,7 Sv (Koesters et al., 2004), in harmony with models of glacial North Atlantic THC, which show that the overturning was weaker or even reversed (Ganopolski et al., 1998). These conclusions are supported by reconstructions of LGM bottom and intermediate water ventilation inferred from epibenthic foraminiferal $\partial^{13}C$ (Curry et al., 1988; Duplessy et al., 1988; Sarnthein et al., 1994; Skinner & Shackleton, 2004) and estimates of deepwater export from the North Atlantic based on foraminiferal Cd/Ca (Boyle 1992) and sediment $^{231}Pa/^{230}Th$ (Yu et al., 1996; McManus et al., 2004). These estimates indicate a major reduction in the flux of North Atlantic Deepwater accompanied by an enhanced northward advection of Antarctic Bottom Water but still remain semi-quantitative, a "major embarrassment" to paleoceanography, as it was stressed at the recent SCOR/IMAGES workshop in Atlanta (March 2005).

Reconstructions of LGM sea ice cover based on sea surface temperature estimates and the spatial pattern of planktic $\partial^{18}O$ revealed that large portions of the glacial Nordic Seas were ice-free during summer (Weinelt et al., 1996; Norgaard-Pedersen et al., 2003; Sarnthein et al., 2003). Accordingly, deepwater continued to form in the Nordic Seas also during the LGM owing to open-ocean convection during interstadials and/or injections of high-salinity brine water during stadials with enhanced seasonal sea ice formation (Dokken & Jansen, 1999; Voelker, 1999). These results are in agreement with the model of Paul & Schaefer-Neth (2003) showing ongoing convection in the Nordic Seas during the LGM and suggest that a minor DSO was flowing into the Northern North Atlantic over most of that time.

1.2 This study

The objective of this thesis is to reconstruct the variability of the DSO for various periods of major climate change: the Last Glacial to H1 transition, the warming at the boundary between Marine Isotope Stage (MIS) 5.2 and MIS 5.1, and for stadial-to-interstadial times in MIS 4 and early MIS 3.

This reconstruction is based on five new stable isotope records obtained from sites to the north and south of the Denmark Strait and includes several published isotope records.
A short overview of the chapters is given below:

Chapter 2: Variability of the Denmark Strait Overflow during the Last Glacial Maximum. A reconstruction of the spatial and temporal variability of the glacial DSO is obtained on the basis of eight epibenthic stable isotope records from core locations to the north and south of the Denmark Strait. Epibenthic $\partial^{18}O$ is used as proxy for bottom water density assuming that bottom water temperatures at the LGM were close to the freezing point all over the study area and thus the temperature effect on foraminiferal $\partial^{18}O$ values was negligible. Epibenthic $\partial^{13}C$ values are used as proxy of bottom water ventilation (Duplessy 1982; Zahn et al., 1986; Curry et al., 1988). LGM stable isotope values from each coring site have been horizontally projected onto two virtual vertical transects crossing the study area from north-east to south-west and from west to east in order to reveal the spatial distribution pattern of paleo-water masses and gradients of bottom water density and ventilation, which allow us to infer the intensity and pathway of the glacial DSO.

Chapter 3 – section A: Methane-driven Late Pleistocene $\partial^{13}C$ minima and Overflow reversals in the southwestern Greenland Sea. Two planktic $\partial^{13}C$ records from a three-sediment core transect running from the northwestern Icelandic slope, across the Blosseville Basin and the eastern Greenland slope reveal coeval events of extreme $\partial^{13}C$ depletion, which have progressively decreased from the eastern Greenland slope toward east. A series of major $\partial^{13}C$ anomalies start in the middle of MIS 5.2 and has a total duration of approximately 18,000 years. Negative planktic $\partial^{13}C$ extremes around –6 ‰ occur during peak DO stadial 22 and subsequent DO interstadial 21 and match a peak in atmospheric methane concentration (Blunier & Brook, 2001). A second major $\partial^{13}C$ event reaching –5 ‰ is documented over 4000 years by both planktic and epibenthic $\partial^{13}C$ records near the onset of DO interstadial 14.

These extreme ^{13}C-depletions reach beyond the natural range of $\partial^{13}C$ in Dissolved Inorganic Carbon (DIC) driven by the remineralization of organic matter.

Thus they cannot be accounted for in terms of nutrient enrichment in ocean water, but rather require an alternative source of light carbon isotope, that is methane released from gas hydrate (clathrate) reservoirs. This hypothesis is also supported by the evidence of a DSO reversal during the meltwater regime of MIS 5.2. During this time strongly reduced sea surface salinity in the Nordic Seas (recorded as planktic $\partial^{18}O$ minimum) induced a strong stratification of the surface ocean, sea ice formation that sealed off the sea surface, and a complete breakdown of deepwater formation in the Nordic Seas, which in turn may have led to a northward incursion of relatively warm (8°C) and saline Atlantic Upper Intermediate Water (Zahn et al., 1987; Rasmussen & Thomsen, 2004) and a bottom water warming by 8 to 9 °C. This warming possibly triggered dissociation of methane hydrates in sediments along the eastern Greenland slope and a release of methane into the Blosseville Basin. A hypothesis is proposed that a plume of methane spread from the East Greenland slope and rapidly diffused toward Iceland. This model is consistent with evidence that the $\partial^{13}C$ excursion was found coeval at two different locations and clearly decreased from west to east. Oxidation of methane (-40 to –60 ‰ $\partial^{13}C$) to isotopically light DIC led to the observed negative $\partial^{13}C$ shift in planktic and benthic foraminiferal tests.

Scanning Electron Microscope (SEM) and light microscope investigations revealed that planktic and benthic foraminifera obtained from the record with maximum negative $\partial^{13}C$ excursion are also affected by a post-depositional, secondary overgrowth of authigenic carbonate which is absent in non-excursion (i.e. $\partial^{13}C$= 0 ‰) intervals. In contrast, foraminifera obtained from the two coring sites more distal from the East Greenland margin, which exhibit minor ^{13}C-depletion, do not show evidence of diagenetic overgrowth under the binocular.

In summary, the negative $\partial^{13}C$ excursions in the western Blosseville Basin possibly reflect a primary and a secondary, methane-induced decrease in $\partial^{13}C_{DIC}$. The authigenic carbonate overcrusts have additionally lowered foraminiferal $\partial^{13}C$ at the site of maximum carbon isotope shift. Most likely they formed in a microenvironment of high methane concentration in pore fluids, which locally caused a supersaturation in isotopically light $CaCO_3$ (discussed in detail in Chapter 3B). Methane may have escaped the sea floor near to this location and may have diffused in the water column slightly eastward in the basin, across the track of the EGC.

Chapter 3 - section B: Methane-induced early diagenesis of foraminiferal tests in the southwestern Greenland Sea. It is a matter of ongoing debate, whether extremely negative foraminiferal $\partial^{13}C$ values that are interpreted to reflect events of clathrate destabilization and subsequent injections of methane into the ocean may either derive from the DIC composition at primary calcification and/or from authigenesis (Torres et al., 2003; Cannariato & Stott, 2004, Hill et al., 2004). Chapter 3B focuses on the relationship between extreme, possibly methane-induced planktic and epibenthic ^{13}C-depletions and features of diagenetic alteration of foraminifera.

SEM and light microscopic evidence revealed that ^{13}C-depleted foraminifera are enveloped by authigenic crusts which amount to 10 to 20 % of the total test, while the remaining 80 to 90 % appears to be unaltered, primary calcite. This feature likewise affects planktic, epi- and endobenthic species and consists of a cryptocrystalline overgrowth on the external walls, whereas cryptocrystals are quasi-prismatic and reach up to 10 µm within the chambers. Porous species as *Neogloboquadrina pachyderma* sinistral are more extensively altered than less porous species such as *Cibicides lobatulus*. Qualitative Electron Dispersive X-rays (EDX) estimates of the elemental composition suggest that the overgrowth consists of calcite enriched in manganese and iron. Foraminifera obtained from core intervals with "normal" (0 ‰) $\partial^{13}C$ values appear largely unaffected by authigenetic alteration under the SEM and do not reveal any enrichment in trace elements.

Two subsamples of *N. pachyderma* s. obtained from one and the same ^{13}C-depleted interval were progressively leached up to 30 and 60 % of the original mass and subsequently analysed in order to reveal potential $\partial^{13}C$ changes. This experiment relied on the assumption that primary and secondary calcite are differentially sensitive to dissolution because of different crystal structures. Thus, differences in the isotopic composition of both components might be inferred from differential post-leaching $\partial^{13}C$ values and a mass balance calculation. It turned out that specimens which underwent leaching revealed slightly more negative $\partial^{13}C$ values than unleached specimens. The mass balance indicated that both the primary *and* the authigenetic component are ^{13}C-depleted, the secondary, possibly authigenic overcrust being isotopically lighter than the original tests. Hence, the $\partial^{13}C$ values of the primary foraminiferal test are likely to document a negative excursion in $\partial^{13}C_{DIC}$, while the $\partial^{13}C$ of the overcrust may reflect the composition of ^{12}C-enriched pore fluids.

Since the organic carbon content of Quaternary sediments at the East Greenland slope is very low (Schlueter et al., 2001), thermal destabilization of clathrates and subsequent release of methane is the most plausible explanation to account for a simultaneous ^{12}C-enrichment in pore fluids and ocean DIC. Oxidation of methane in seawater may have driven a negative shift of $\partial^{13}C_{DIC}$, whereas pore water methane may have led to supersaturation of isotopically light calcium carbonate which eventually precipitated on and in foraminifera tests (in case the observed crusts do not partially belong to the encrustations that are characteristic of *N. pachyderma* s. that have reached an adult stage in the water column).

1.3 Materials and methods

Today the DSO cascades down to the south of the Denmark Strait to more than 2500 m water depth and flows along the western basin margin, directly adjacent to the continental slope of East Greenland (Dickson & Brown, 1994). From this location we obtained epibenthic and planktic stable isotope records from five sediment cores, where Late Quaternary sedimentation was expected to have been little disturbed by erosion (Fig. 1, Table 1). The coring sites are located along a north-to-south transect that parallel the DSO flow line in order to monitor its temporal and spatial variability.

Core PS62/015-3 (980 m water depth) was obtained to the north of the Denmark Strait from the western margin of the Blosseville Basin, core PS62/017-4 (1458 m water depth) was retrieved from the central basin floor. Both sites today are bathed in peripheral DSO below extensive sea ice and frequent icebergs characteristic of the domain of the East Greenland Current. Site GIK23519 (1893 m water depth) is located off the southern outlet of the Denmark Strait and today lies to the east of the DSO pathway, under the influence of a distal branch of the Iceland-Scotland Overflow. Sites PS62/003-2 (2159 m water depth) and PS62/004-3 (2565 m water depth) lie on a transect crossing the southeastern Greenland margin and are located where the DSO gradually merges into North Atlantic Deepwater.

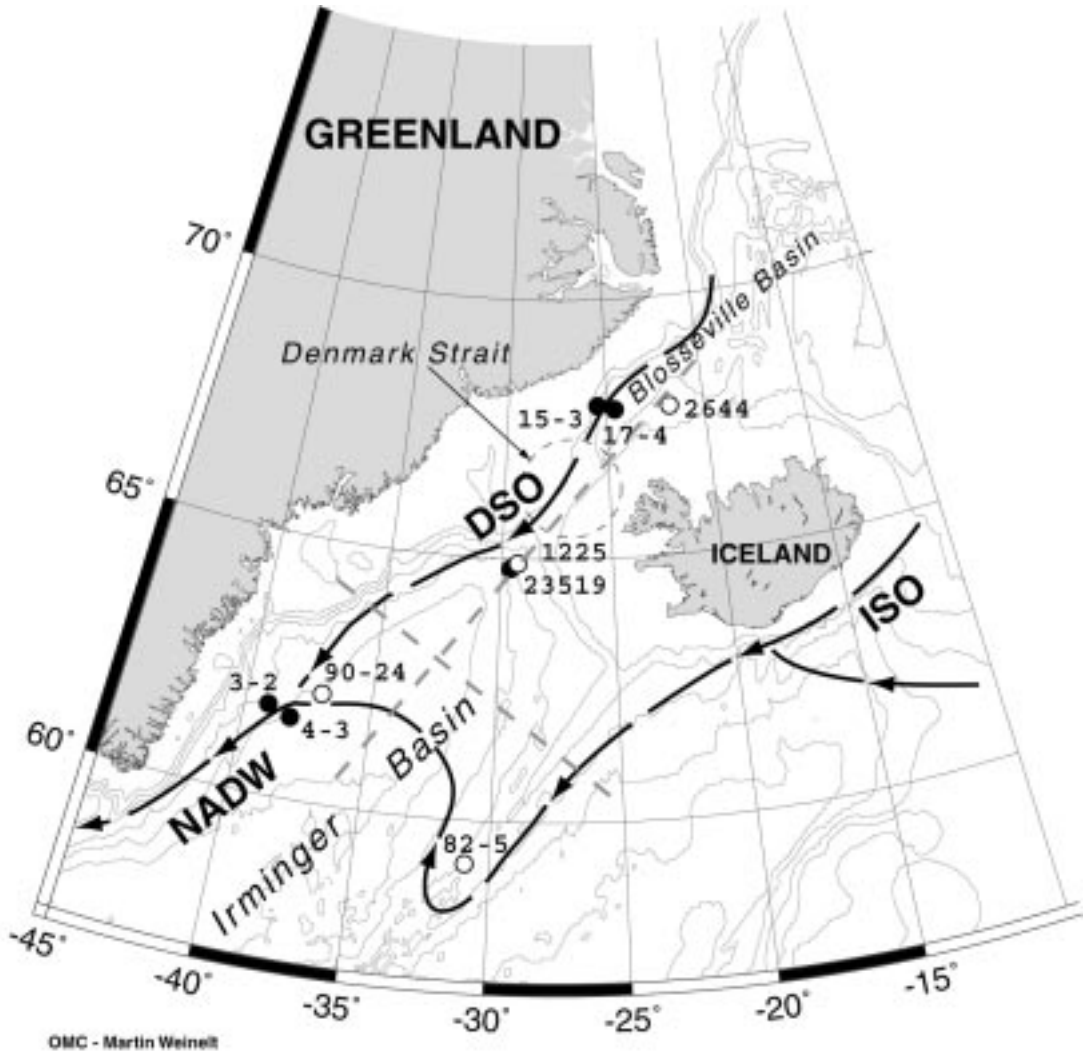

Fig. 1. Location of new (filled circles) and published (open circles) sediment records presented in this study. Black dashed lines schematically represent the modern bottom current system in the study area. DSO = Denmark Strait Overflow; ISO = Iceland-Scotland Overflow; NADW = North Atlantic Deepwater. Stable isotope values have been ideally projected from each core location onto virtual transects (grey dashed lines) to reconstruct the variability of the DSO during the Last Glacial Maximum. Published records are: Site SU 90-24 (Elliot et al., 2002); Site SO 82-5 (Jung, 1996; van Kreveld et al., 2000); Site JM96-1225 (Hagen & Hald, 2002); Site PS2644 (Voelker et al., 1998)

Core	Recovery (m)	Latitude	Longitude	Water depth (m)	Average sedimentation rate (cm/kyrs)	Average sampling resolution (cm)	Average sampling resolution (yrs)
PS62/015-3	6.36	67° 55.855' N	25° 25.590' W	980	7	2	280
PS62/017-4	6.32	67° 51.014' N	24° 35.116' W	1458	8	2	260
GIK 23519	6.41	64° 47.840' N	29° 35.750' W	1893	6	2	300
PS62/003-2	12.40	61° 42.003' N	39° 04.041' W	2159	11	6	550
PS62/004-3	12.96	61° 31.559' N	38° 07.387' W	2565	12.5	10	800

Table 1. New sediment records presented in this study

The work halves of the sediment cores were sampled centimeter-wise. Sediment samples were washed over a 63-µm sieve and dried at 40 °C. Where available, 25 specimens of *N. pachyderma* s. (150-250 µm) and 1 to 10 specimens of *C. wuellerstorfi* or *C. lobatulus* (250-400 µm) were hand-picked for multiple and

single-specimen stable isotope analysis respectively. According to standard preparation routine, foraminifera were cleansed in ethanol, gently crushed and treated for 10 seconds in the ultrasonic bath. After vigorous ultrasonic shaking, undesired fine carbonate debris, coccoliths, and other potential contaminants go into suspension and may easily be eliminated by decanting the ethanol from the vial. Oxygen and carbon stable isotope values were measured at the Leibniz Laboratory of Kiel University using the Carboprep line and an automated MAT-251 mass spectrometer (analytical precision: ± 0.07 ‰ for $\partial^{18}O$, ± 0.05 ‰ for $\partial^{13}C$). Stable isotope data (altogether 1532 measurements) are being stored at PANGAEA databank.

Epibenthic $\partial^{18}O$ values were adjusted to $\partial^{18}O$ values of *Uvigerina peregrina* by adding 0.64 ‰ and used as proxy for bottom water density, assuming that sea bottom temperature at the LGM was close to the freezing point and the temperature effect on $\partial^{18}O$ changes can thus be ignored. Epibenthic $\partial^{13}C$ values, in turn, were used as proxy for bottom water ventilation (Duplessy, 1982; Zahn et al., 1986, Curry et al., 1988). We did not apply the +0.32 ‰ correction to glacial $\partial^{13}C$ values because they would exceed the maximum $\partial^{13}C$ value of 2 ‰ resulting from physical fractionation at the atmosphere-ocean interface.

Analysis of single-grain benthic foraminifera makes it possible to determine the short-term variability of $\partial^{18}O$ and $\partial^{13}C$ values within each sample interval. This variability may reveal whether some benthic foraminifera specimens calcified under the influence of high salinity, dense brine water (Voelker, 1999) which is released near to the sea surface during (seasonal) sea ice formation and is distinguished by light $\partial^{18}O$ /$\partial^{13}C$ signals at the sea floor (Veum et al., 1992). Furthermore, single-specimen isotope data provide information about the range of absolute maximum and minimum $\partial^{18}O$ and $\partial^{13}C$ values which document maxima and minima in bottom water density and ventilation. This information is averaged out by using multiple-specimens analyses.

The degree of (possibly methane-induced) diagenetic alteration of planktic and benthic foraminifera at Site PS62/015-3 was assessed under the binocular with up to a 32 X magnification and with SEM. Qualitative estimates of the trace element composition of the tests were obtained by EDX (CAMSCAN Serie 2 CS 44). Foraminiferal specimens were fixed on a stub and subsequently coated with a mixture of gold and palladium to improve backscatter.

SAMPLES PREPARATION PROCEDURE

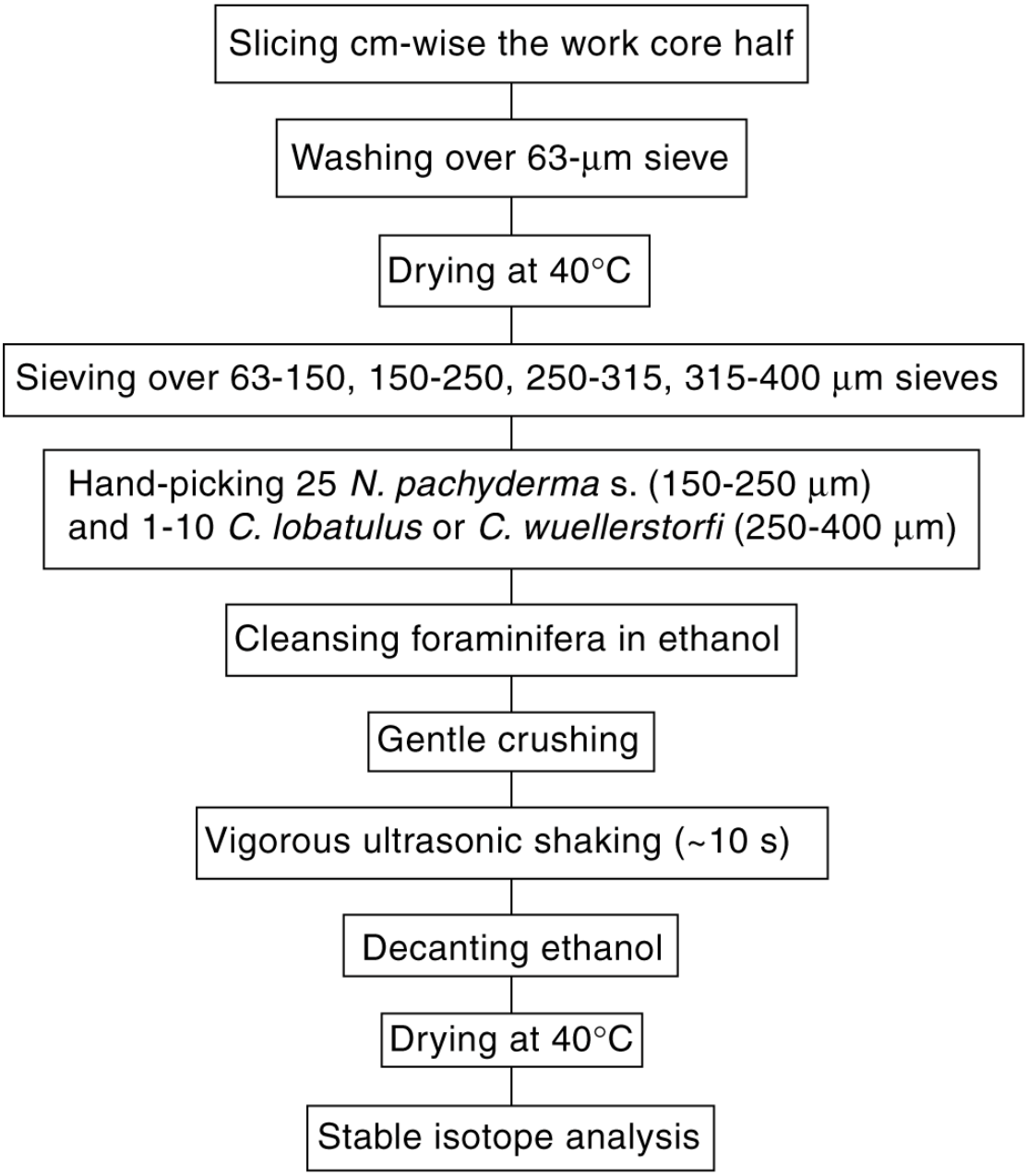

1.4 Age control

The chronology of cores PS62/015-3 and PS62/017-4 is based on both $\partial^{18}O$ and magnetic stratigraphy. Correlation of relative paleointensity and inclination with the North Atlantic reference record NAPIS 75 (Laj et al., 2000) provided the chronostratigraphic framework for the last 75 kyrs. Norwegian Basin (65 kyrs), Laschamp (41 kyrs), and Mono Lake (34.5 kyrs) events of minimum magnetic intensity served as major correlation markers. On the basis of this magneto-stratigraphic framework planktic $\partial^{18}O$ records of cores PS62/015-3 and PS62/017-4 were tuned to the high-resolution planktic $\partial^{18}O$ record of neighbour core PS2644 the chronology of which is based on densely-spaced ^{14}C datings and on tuning to the incremental time scale of GISP2 (Voelker et al., 1998). Abrupt light $\partial^{18}O$ spikes in core PS2644 are accompanied by high percentages of ice-rafted debris and increased percentages of *N. pachyderma* s., indicative of low sea surface temperature (Voelker et al., 1998). Accordingly, these planktic $\partial^{18}O$ peaks are considered to reflect meltwater pulses of Heinrich Events 1 to 6 and other cold DO stadials in GISP2 (Bond et al., 1993), meltwater pulses that spread far across the East Greenland continental margin. Conversely, the end of each meltwater spike in the planktic $\partial^{18}O$ record of core PS2644 was matched to phases of abrupt temperature rise on Greenland.

The transition from the LGM to H1 is identified on the basis of a prominent planktic $\partial^{18}O$ shift from 4.5 to 2.5 ‰ in the uppermost sections of cores PS2644, PS62/015-3, and PS62/017-4. This shift forms a fundamental correlation marker between the three planktic $\partial^{18}O$ records. Other major correlation markers are the meltwater spikes corresponding to stadials such as Heinrich Events 3 (MIS 2/ MIS 3 boundary), H4, H5, H5.2, and H6 (MIS 3/ MIS 4 boundary). Since the chronology of core PS2644 is tuned to GISP2, we used the GISP2 time scale (Grootes & Stuiver, 1997) as stratigraphic reference for MIS 3 and 4, whereas the lowermost portions of the records were dated according to the North GRIP time scale (North Greenland Ice Core Project Members 2004). The record of core PS62/015-3 reaches back to 86.5 kyrs, the center of MIS 5.2, whereas the record of core PS62/017-4 reaches MIS 5.1, back to 78 kyrs.

The age control of core GIK23519 is based on $\partial^{18}O$ stratigraphy and five ^{14}C datings for the interval spanning the LGM and Terminations IA and IB (Fig. 2; Table 2). Because of poor preservation of this gravity core near its top, we correlated the upper section of the planktic $\partial^{18}O$ record with a record from a box corer retrieved at the same location and produced a composite depth record for the Holocene.

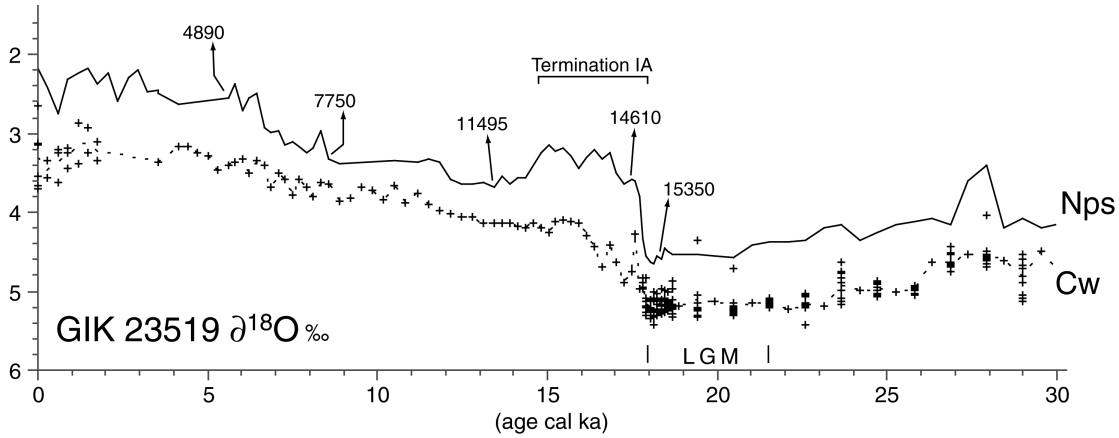

Fig. 2. Planktic and epibenthic $\partial^{18}O$ records of Site 23519 plotted versus calendar age. LGM defined according to GLAMAP 2000 (Sarnthein et al., 2003). Arrows indicate positions of ^{14}C ages. A reservoir effect correction of –400 yrs has been applied to all ^{14}C ages. Nps = *Neogloboquadrina pachyderma* sin.; Cw = *Cibicidoides wuellerstorfi.*

Sample	Core composite depth (cm)	Species	Size fract. (µm)	weight (mg)	^{14}C-age (yrs)
KIA 582	20	*C. bulloides*	315-400	9.6	4890 ±40
KIA 583	34	*C. bulloides*	315-400	7.3	7750 ±50
KIA19050	49	*N.pachyderma* sin.	150-250	14.7	11495 ±60
KIA19051	67	*N.pachyderma* sin.	150-250	9.5	14610 ±80
KIA19052	75	*N.pachyderma* sin.	150-250	12.2	15350 ±90

Table 2. ^{14}C datings in core 23519.

A plateau of constant maximum planktic $\partial^{18}O$ values of 4.5 to 4.7 ‰ and benthic $\partial^{18}O$ values of 5.2 to 5.4 ‰ (Fig. 2) forms a most prominent stratigraphic marker in GIK23519, which corresponds to the LGM according to the definition ("Last Isotopic Maximum") given by GLAMAP 2000 (Sarnthein et al., 2003). The end of the LGM is characterized by an abrupt decrease in planktic $\partial^{18}O$ to values of 3.5 ‰, which is paralleled by a distinct drop of benthic $\partial^{18}O$ values from 5.3 to 4.25 ‰. The latter may be partly interpreted as brine water signal resulting from enhanced sea ice formation during H1 (Fig. 2). The Holocene is characterized by a gradual decrease of benthic and planktic $\partial^{18}O$ values, interrupted by minor meltwater signals in the planktic record.

The age models of cores PS62/003-2 and PS62/004-3 are based on correlation of epibenthic $\partial^{18}O$ records with the densely ^{14}C-dated epibenthic $\partial^{18}O$ record of neighbour core SU90-24 (Elliot et al., 1998; Elliot et al., 2002).

For reasons of internal consistency we converted all ^{14}C ages older than 13,000 years into calendar ages after Voelker et al. (1998) after deducing a global reservoir age of – 400 years. However, Waelbroeck et al. (2001) demonstrated that the reservoir age near the top of H1 (15 kyrs BP) was ~1800 years, whereas it was ~800 years at the end of the Younger Dryas cold event (approximately 11.6 kyrs BP). Accordingly, the timing of H1 in our age model may be overestimated by up to 1.4 kyrs.

Correlation of foraminiferal $\partial^{18}O$ records and magnetic intensities was carried out by using the software AnalySeries, version 1.2 (Paillard et al., 1996). In summary, planktic $\partial^{18}O$ records of cores PS62/015-3 and PS62/017-4 correlate with those of core PS2644 with a squared correlation coefficient r^2= 0.40 and 0.60 respectively. r^2= 0.56 and 0.58 for the correlation between benthic $\partial^{18}O$ records of cores PS62/003-2 and PS62/004-3 versus SU90-24. Discrepancies are mainly due to a lower sampling resolution of cores PS62/015-3 and PS62/017-4, and scarcity of epibenthic foraminifera in various sections of cores PS62/003-2 and PS62/004-3.

References for Chapter 1

Blunier, T. & Brook, E.J. 2001: Timing of millennial-scale climate change in Antarctica and Greenland during the last glacial period. *Science 291*, 109-112.

Bond, G., Broeker, W., Johnsen, S., McManus, J., Labeyrie, L., Jouzel, J. & Bonani, G. 1993: Correlations between climate records from North Atlantic sediments and Greenland ice. *Nature 365*, 143-147.

Boyle, E.A. 1992: Cadmium and $\partial^{13}C$ paleochemical ocean distributions during the stage 2 glacial maximum. *Annual Reviews Earth Planetary Science 20*, 245-287.

Cannariato, K.G. & Stott, L.D. 2004: Evidence against clathrate-derived methane release to Santa Barbara Basin surface waters? *Geochemistry Geophysics Geosystems 5*, doi. 10.1029/2003GC000600.

Curry, W.B., Duplessy, J.C., Labeyrie, L.D. & Shackleton, N.J. 1988: Changes in the distribution of $\partial^{13}C$ of deep water ΣCO_2 between the last glaciation and the Holocene. *Paleoceanography 3*, 317-341.

Dickson, R.R. & Brown, J. 1994: The Production of North Atlantic Deep Water – Sources, Rates and Pathways. *Journal of Geophysical Research C99*, 12319-12341.

Dickson, B., Yashayaev, I., Meincke, J., Turrell, B., Dye, S. & Holfort, J. 2002: Rapid freshening of the deep North Atlantic Ocean over the past four decades. *Nature 416*, 832-837.

Dokken, T.M. & Jansen, E. 1999: Rapid changes in the mechanism of ocean convection during the last glacial cycle. *Nature 401*, 458-461.

Duplessy, J.-C. 1982: North Atlantic Deep Water circulation during the last climatic cycle. *Bulletin Institut de Geólogie de Bassin d'Aquitaine 31*, 379-391.

Duplessy, J.-C., Shackleton, N.J., Fairbanks, R.G., Labeyrie, L., Oppo, D. & Kallel, N. 1988: Deepwater source variations during the last climatic cycle and their impact on the global deepwater circulation. *Paleoceanography 3*, 343-360.

Elliot, M., Labeyrie, L., Bond, G., Cortijo, E., Turon, J.L., Tisnerat, N. & Duplessy, J.-C. 1998: Millennial-scale iceberg discharges in the Irminger Basin during the last glacial period: Relationship with the Heinrich events and environmental settings. *Paleoceanography 13*, 433-466.

Elliot, M., Labeyrie, L. & Duplessy, J.-C. 2002: Changes in North Atlantic deep-water formation associated with the Dansgaard-Oeschger temperature oscillations (60-10 ka). *Quaternary Science Reviews 21*, 1153-1165.

Fleming, K. & Lambeck, K. 2004: Constraints on the Greenland Ice Sheet since the Last Glacial Maximum from sea-level observations and glacial-rebound models. *Quaternary Science Reviews 23*, 1053-1077.

Ganopolski, A., Rahmstorf, S., Petoukhov, V. & Claussen, M. 1998: Simulation of modern and glacial climates with a coupled global model of intermediate complexity. *Nature 391*, 351-356.

Grootes, P.M. & Stuiver, M. 1997: $^{18}O/^{16}O$ variability in Greenland snow and ice with 10^{-3} to 10^{5} year time resolution. *Journal of Geophysical Research 102*, 26455-26470.

Hagen, S. & Hald, M. 2002: Variation in surface and deep water circulation in the Denmark Strait, North Atlantic, during marine isotope stages 3 and 2. *Paleoceanography 17*, 1-16.

Hansen, B. & Østerhus, S. 2000: North Atlantic-Nordic Seas exchanges. *Progress in Oceanography 45*, 109-208.

Hansen, B., Turell, W.R. & Østerhus, S. 2001: Decreasing overflow from the Nordic Seas into the Atlantic Ocean through the Faeroe-Shetland Channel since 1950. *Nature 411*, 927-930.

Hill, T.M., Kennett, J.P. & Spero, H.J. 2004: High-resolution records of methane hydrate dissociation: ODP Site 893, Santa Barbara Basin. *Earth and Planetary Science Letters 223*, 127-140.

Hill, T.M., Kennett, J.P. & Valentine, D.L. 2004: Isotopic evidence for the incorporation of methane-derived carbon into foraminifera from modern methane seeps, Hydrate Ridge, Northeast Pacific. *Geochimica et Cosmochimica Acta 68*, 4619-4627.

Jung, S. 1996: Wassermassenaustausch zwischen NE-Atlantik und Nordmeer waehrend der letzen 300,000/ 80,000 Jahre im Abbild stabiler O- und C-Isotope. *Berichte aus dem Sonderforschungsbereich 313 nr. 61*, University of Kiel, 104 pp.

Koesters, F., Kaese, R., Fleming, K. & Wolf, D. 2004: Denmark Strait overflow for Last Glacial maximum to Holocene conditions. *Paleoceanography 19*, PA2019.

Laj, C., Kissel, C., Mazaud, A., Channell, J.E.T. & Beer, J. 2000: North Atlantic paleointensity stack since 75 ka (NAPIS-75) and the duration of the Laschamp event. *Royal Society of London Philosophical Transactions, ser. A vol. 358*, 1009-1025.

Lambeck, K. & Chappell, J. 2001: Sea level change through the last glacial cycle. *Science 292*, 679-686.

Larsen, B. 1983: Geology of the Greenland-Iceland Ridge in the Denmark Strait. *In* Bott, M.H.P., Saxov, S., Talwani, M. & Thiede, J. (eds.): *Structure and Development of the Greenland-Scotland Ridge: New Methods and Concepts*, 425-444. Plenum Press, New York.

McManus, J.F., Francois, R., Gheradi, J.M., Keigwin, L.D. & Brown-Leger, S. 2004: Collapse and rapid resumption of Atlantic meridional circulation linked to deglacial climate changes. *Nature 428*, 834-837.

Norgaard-Pedersen, N., Spielhagen, R.F., Erlenkeuser, H., Grootes, P.M., Heinemeier, J. & Knies, J. 2003: Arctic Ocean during the Last Glacial Maximum: Atlantic and polar domains of surface water mass distribution and ice cover. *Paleoceanography 18*, 8.

North Greenland Ice Core Project members 2004: High-resolution record of Northern Hemisphere climate extending into the last interglacial period. *Nature 431*, 147-151.

Paillard, D., Labeyrie, L. & Yiou, P. 1996: Macintosh program performs time-series analysis. *EOS Transactions American Geophysical Union 77*, 379.

Paul, A. & Schäfer-Neth, C. 2003: Modeling the water masses of the Atlantic Ocean at the last Glacial Maximum. *Paleoceanography 18*, 3.

Rasmussen, T.L. & Thomsen, E. 2004: The role of the North Atlantic Drift in the millennial timescale glacial climate fluctuations. P*alaeogeography, Palaeoclimatology, Palaeoecology 210*, 101-116.

Sarnthein, M., Pflaumann, U. & Weinelt, M. 2003: Past extent of sea ice in the northern North Atlantic inferred from foraminiferal paleotemperature estimates. *Paleoceanography 18*, 1-8.

Sarnthein, M., Winn, K., Jung, S.J.A., Duplessy, J.-C., Labeyrie, L., Erlenkeuser, H. & Ganssen, G. 1994: Changes in east Atlantic deepwater circulation over the last 30,000 years: Eight time slice reconstructions. *Paleoceanography 9*, 209-267.

Schlueter, M., Sauter, E.J., Schulz-Bull, D., Balzer, W. & Suess, E. 2001: Fluxes of organic carbon and biogenic silica reaching the seafloor: A comparison of high northern and southern latitudes of the Atlantic Ocean. *In* Schaefer, P. et al. (eds.): *The Northern North Atlantic: A changing environment*, 225-240. Springer, Berlin.

Skinner, L.C. & Shackleton, N.J. 2004: Rapid transient changes in the northeast Atlantic deep water ventilation age across termination I. *Paleoceanography 19*, PA 2005.

Torres, M.E., Mix, A.C., Kinports, K., Haley, B., Klinkhammer, G.P., McManus, J. & de Angelis, M.A. 2003: Is methane venting at the seafloor recorded by $\partial^{13}C$ of benthic foraminifera shells? *Paleoceanography 18*, 1062.

van Kreveld, S., Sarnthein, M., Erlenkeuser, H., Grootes, P., Jung, S., Nadeau, M.J., Pflaumann, U. & Voelker, A. 2000: Potential links between surging ice sheets, circulation changes, and the Dansgaard-Oeschger cycles in the Irminger Sea, 60-18 kyr. *Paleoceanography, 15*, 425-442.

Veum, T., Jansen, E., Arnoldt, M., Beyer, I. & Duplessy, J.-C. 1992: Water mass exchange between the North Atlantic and the Norwegian Sea during the past 28.000 years. *Nature 356*, 783-785.

Voelker, A.H. 1999: Zur Deutung der Dansgaard-Oeschger Ereignisse in ultra-hochauflösenden Sedimentprofilen aus dem Europäischen Nordmeer. *Ph.D. thesis*, University of Kiel, 180 pp.

Voelker, A. H., Sarnthein, M., Grootes, P.M., Erlenkeuser, H., Laj, C., Mazaud, A., Nadeau, M. J. & Schleicher, M. 1998: Correlation of marine ^{14}C ages from the Nordic Seas with the GISP2 isotope record: implications for ^{14}C calibration beyond 25 ka BP. *Radiocarbon 40*, 517-534.

Waelbroeck, C., Duplessy, J.-C., Michel, E., Labeyrie, L., Paillard, D. & Duprat, J. 2001: The timing of the last deglaciation in North Atlantic climate records. *Nature 412*, 724-726.

Weinelt, M., Sarnthein, M., Pflaumann, U., Schulz, H., Jung, S. & Erlenkeuser, H. 1996: Ice-free Nordic Seas during the Last Glacial Maximum? Potential sites of deepwater formation. *Paleoclimate 1*, 283-309.

Whitehead, J.A., Leetmaa, A. & Knox, R.A. 1974: Rotating hydraulics of strait and sill flows. *Geophysical Fluid Dynamics 6*, 101-125.

Yu, E.-F., Francois, R. & Bacon, M.P. 1996: Similar rates of modern and last-glacial ocean thermohaline circulation inferred from radiochemical data. *Nature 379*, 689-694.

Zahn, R., Sarnthein, M. & Erlenkeuser, H. 1987: Benthos isotopic evidence for changes of the Mediterranean outflow during the late Quaternary. *Paleoceanography 2*, 543-559.

Zahn, R., Winn, K. & Sarnthein, M. 1986: Benthic foraminiferal $\partial^{13}C$ and accumulation rates of organic carbon: *Uvigerina peregrina* group and *Cibicidoides wuellerstorfi*. *Paleoceanography 1*, 27-42.

CHAPTER 2

Variability of the Denmark Strait Overflow during the Last Glacial Maximum

CHRISTIAN MILLO, MICHAEL SARNTHEIN, ANTJE VOELKER AND HELMUT ERLENKEUSER

Christian Millo (cm@gpi.uni-kiel.de) and Michael Sarnthein, Department of Geology, Christian-Albrechts-Universitaet, Olshausenstrasse 40, D-24118 Kiel, Germany;

Antje Voelker, INETI Department of Marine Geology, Estrada da Portela, Zambujal, 2720 Alfragide, Portugal;

Helmut Erlenkeuser, Leibniz-Labor for Radiometric Dating and Isotope Research, Max-Eyth-Strasse 11, D-24118 Kiel, Germany.

Accepted for publication in *Boreas* on 28 July 2005

Abstract

The Denmark Strait Overflow (DSO) today compensates for the northward flowing Norwegian and Irminger branches of the North Atlantic Current that drive the Nordic heat pump. During the Last Glacial Maximum (LGM) ice sheets constricted the Denmark Strait aperture in addition to ice eustatic/isostatic effects which reduced its depth (today ~630 m) by ~130 m. These factors combined with a reduced north-south density gradient of the water masses are expected to have restricted or even reversed the LGM DSO intensity. To better confine these boundary conditions, we present a first reconstruction of the glacial DSO, using four new and four published epibenthic and planktic stable-isotope records from sites to the north and south of the Denmark Strait. The spatial and temporal distribution of epibenthic $\delta^{18}O$ and $\delta^{13}C$ maxima reveals a north-south density gradient at intermediate water depths from σ_0 ~28.7 to 28.4 / 28.1 and suggests that dense and highly ventilated water was convected in the Nordic Seas during the LGM. On the other hand, extremely high epibenthic $\delta^{13}C$ values on top of the Mid Atlantic Ridge document a further convection cell of Glacial North Atlantic Intermediate Water to the south of Iceland, which however was

marked by much lower density (σ_0 ~28.1). The north-south gradient of water density possibly implied that the glacial DSO was directed to the south like today and fed Glacial North Atlantic Deepwater that has underthrusted the Glacial North Atlantic Intermediate Water in the Irminger Basin.

2.1 Introduction

The Denmark Strait, together with the Iceland-Faeroe and the Faeroe-Shetland Channel today form the most important gateway for meridional ocean circulation in the northern hemisphere (Dickson & Brown 1994). Deepwater originating from winter convection in the Nordic Seas forms huge currents of cold and dense water, which cross these passages and cascade into the northern North Atlantic, compensating for the northward inflow of relatively warm and saline surface water carried by the North Atlantic Current and its ramifications. Hansen & Østerhus (2000) calculated that the Norwegian and Greenland Seas today receive a total flux of approximately eight Sverdrups (Sv), that is 8 x 10^6 m^3/s, advected by the North Atlantic Current and its branches (Fig. 1). The Arctic Ocean receives an additional flux of 1 Sv from the Pacific Ocean via the Bering Strait. This inflow is balanced by the outflow across the Canadian Archipelago (1.7 Sv), along the eastern Greenland shelf (East Greenland Current, 1.3 Sv), and at intermediate depths by the Iceland-Shetland Overflow (3 Sv) and the Denmark Strait Overflow (DSO) (3 Sv) (Fig. 1). This mass balance is a key factor governing the poleward heat transport in the northern hemisphere and has a strong influence on the climate in Europe and total Eurasia.

The DSO has particular climatic relevance in that it may influence the intensity of North Atlantic Deep Water (NADW) circulation (Gerdes & Köberle 1995; Dickson *et al.* 1997; Dörscher & Redler 1997). The strength of DSO mainly depends on the density gradient between water masses to the north and south of the Denmark Strait and the height of dense water above the strait's sill (Whitehead *et al.* 1974). Variations in density contrast may arise from episodic meltwater discharge from sea ice and nearby ice sheets. It has recently been shown that the density σ_0 of DSO diminished by about 0.02 over the last forty years due to a 0.035‰ salinity decrease (Dickson *et al.* 2002). This freshening was accompanied by a 20% decrease in the Faeroe component of the Overflow (Hansen *et al.* 2001). South of the Denmark Strait

the DSO cascades down to more than 2500 m water depth, forming a major source of NADW (Fig. 2).

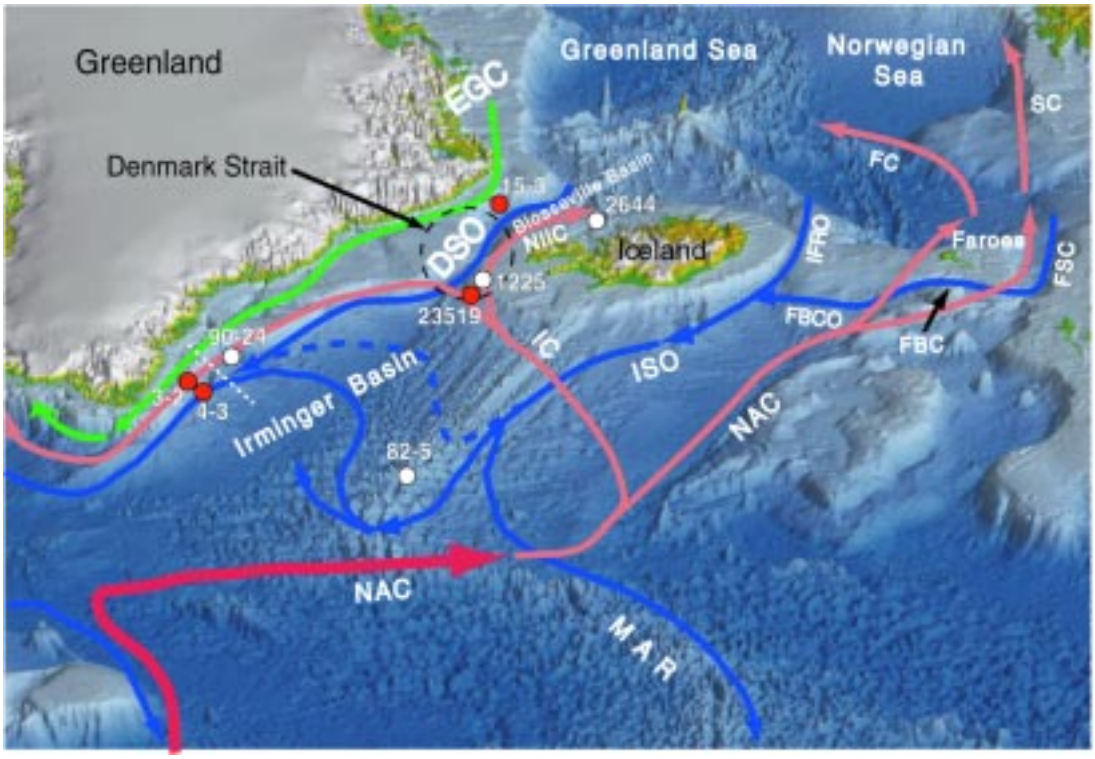

Fig. 1. Location of core sites and schematic surface and deepwater circulation in the Nordic Seas (modified from Hansen & Østerhus 2000). Red and white dots respectively indicate locations of new and published stable-isotope records presented in this study. Red arrows = warm surface currents, green arrows = cold surface currents, blue arrows = cold deep currents. NAC = North Atlantic Current; IC = Irminger Current; NIIC = North Icelandic Irminger Current; SC = Shetland Current; FC = Faeroe Current; FBCO = Faeroe Bank Channel Overflow; IFRO = Iceland-Faeroe Ridge Overflow; ISO = Iceland-Scotland Overflow; DSO = Denmark Strait Overflow; EGC = East Greenland Current; FSC = Faeroe-Shetland Channel; FBC = Faeroe Bank Channel; MAR = Mid-Atlantic Ridge. White dashed line indicates position of the transect illustrated in Fig. 2.

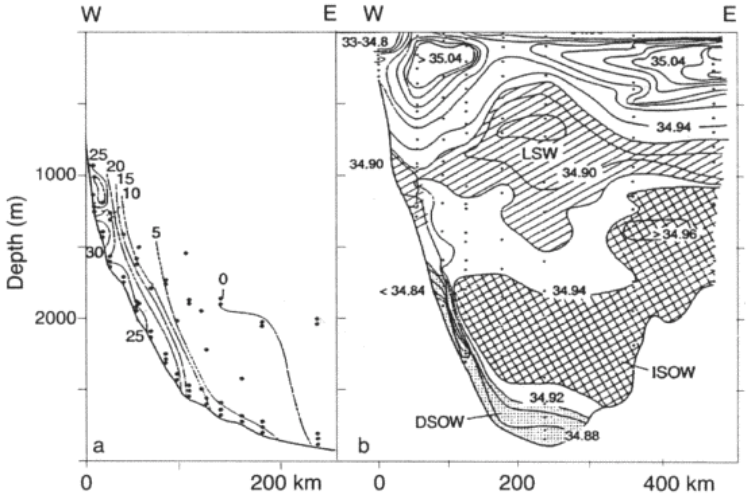

Fig. 2. Westnorthwest to eastsoutheast running transect (see also Fig. 1) indicating the modern distribution of maximum mean near-bottom current velocities (cm/s) (left panel) and water mass salinity (right panel) across the Southeastern Greenland margin and Irminger Basin after Dickson & Brown (1994), as reported in Kuijpers *et al.* (2003). Note the DSO flow at the basin floor in front of the southeastern Greenland slope 2500-2800 m water depth.

Even more severe changes in Overflow intensity are expected to have occurred on geological time scales, with interesting consequences on Atlantic thermohaline circulation (THC) and global climate. During the last glacial period the Denmark Strait sill depth varied significantly, in response to eustatic sea level reduction by 120 to 130 m (Peltier 1994; Lambeck & Chappell 2001; Clark & Mix 2002) and glacio-eustatic rebounds induced by changes in the volume of continental ice sheets in Greenland and Iceland (Fleming & Lambeck 2004). Accordingly, the maximum sill depth of the Denmark Strait (today 630 m) was reduced by about 130 m. In addition, ice sheets on the Greenland and Icelandic shelves (Larsen 1983) constricted considerably the Denmark Strait aperture from both sides. Accordingly, one may expect that the intensity of DSO during the Last Glacial Maximum (LGM) was reduced. Numerical models employed to simulate the strength of NADW formation produce results that appear still inconsistent since the hydrological cycle is poorly represented (Joussaume & Taylor 2000). Some models indeed show that the LGM North Atlantic THC was weaker or reversed (Ganopolski *et al.* 1998; Prange *et al.* 2002; Schmittner *et al.* 2002; Kim *et al.* 2003). Koesters *et al.* (2004) locally constrained the glacial DSO to trickling 0.7 Sv. In contrast, other models even suggest an invigorated glacial overturning (i.e. Kitoh *et al.* 2001; Hewitt *et al.* 2003).

Most empiric reconstructions of bottom and intermediate water ventilation during the LGM were based on epibenthic foraminifera $\delta^{13}C$ and point to a major reduction in glacial NADW formation accompanied by a far northward intrusion of Antarctic Bottom Water (Curry *et al.* 1988; Duplessy *et al.* 1988; Sarnthein *et al.* 1994; Skinner & Shackleton 2004). These results are in harmony with estimates of deepwater export from the North Atlantic based on foraminiferal Cd/Ca (Boyle 1992) and sediment $^{231}Pa/^{230}Th$ records (Yu *et al.* 1996; McManus *et al.* 2004). Various model simulations suggest that the LGM convection cells were located to the south of the Greenland-Scotland Ridge (Ganopolski *et al.* 1998), since CLIMAP (1981) had reconstructed a perennial sea ice cover for the Nordic Seas during glacial times. However, Weinelt *et al.* (1996), Sarnthein *et al.* (2003), and Nørgaard-Pedersen *et al.* (2003) demonstrated that the peak glacial Nordic Seas were largely ice-free during summer. In harmony with these findings, Voelker (1999) and Dokken & Jansen (1999) showed that deepwater formed more or less continuously in the Nordic Seas over the last 60 to 10 kyr, driven by two different mechanisms, open-ocean

convection during interstadials and/or brine rejection during stadials. This conclusion is supported by the model of Paul & Schäfer-Neth (2003), suggesting ongoing LGM convection in the Nordic Seas.

In this paper, we present a detailed reconstruction of the variability of the DSO for the LGM. We present bottom and intermediate water flow directions through the Denmark Strait and potential sources of deepwater on the basis of four new and four published benthic foraminifera stable-isotope records obtained from sediment cores retrieved to the north and south of the Denmark Strait (Fig. 1). Two core sites today lie below the Irminger Current, the other coring sites lie below the EGC and are bathed in peripheral DSO.

2.2 Materials and methods

To trace the spatial and temporal variability of the DSO we obtained epibenthic and planktic stable-isotope records from four sediment cores retrieved along the eastern margin of the path of the Overflow (Fig. 1; Table 1). Site PS62/015-3 (henceforth referred to as site/core 15-3) is located at the East Greenland slope north of the Denmark Strait, Site GIK23519 (henceforth 23519) lies at the southern outlet of the strait, whereas Sites PS62/003-2 and PS62/004-3 (henceforth 3-2 and 4-3) lie on a transect crossing the south-eastern Greenland margin. We also included data from Site PS2644 (henceforth 2644) on the north-western slope of Iceland (Voelker 1999) and published data of cores JM96-1225 (henceforth 1225) (Hagen & Hald 2002), SU90-24 (henceforth 90-24) (Elliot *et al.* 2002), and SO82-5 (henceforth 82-5) (Jung 1996; van Kreveld *et al.* 2000) to establish palaeoceanographic transects across the Irminger Basin.

Table 1. New sediment records presented in this study

Core	Recovery (m)	Latitude	Longitude	Water depth (m)	Average sampling resolution (cm)
PS62/015-3	6.36	67° 55.855' N	25° 25.590' W	980	5
GIK 23519	6.41	64° 47.840' N	29° 35.750' W	1893	1 to 5
PS62/003-2	12.40	61° 42.003' N	39° 04.041' W	2159	10
PS62/004-3	12.96	61° 31.559' N	38° 07.387' W	2565	5 to 10

Sediment cores were sampled in slices 1 cm thick. Samples were washed over a 63-µm sieve and dried at 40°C. Where available 25 specimens of the planktic foraminifera *Neogloboquadrina pachyderma* sinistral (Nps) (150-250 µm) and 1 to 10 specimens of the epibentic *Cibicidoides wuellerstorfi*, *Cibicides lobatulus*, and

Cibicidoides pachyderma (250-400 µm) were hand-picked for multi- and single-specimen stable-isotope analyses. Isotopic data of core 2644 are from Voelker (1999).

Where possible, stable-isotope analyses were carried out on single benthic foraminifera. This method makes it possible to distinguish populations of specimens which calcified their shells in "normally" convected deepwater from shells under the influence of brine water, which therefore are characterized by lighter carbon and oxygen isotopic values. Due to the low weight of epibenthic foraminifera at Sites 3-2 and 4-3, most benthic isotope data were based on analyses of 2 to 3 specimens. A number of core sections were barren of any benthic foraminifera specimens.

Foraminiferal samples were gently crushed, ultrasonically cleaned in ethanol, and dried. Oxygen and carbon stable-isotopes were measured at the Leibniz Laboratory of Kiel University using the Kiel Carboprep line and an automated MAT-251 mass spectrometer (analytical precision: ± 0.07‰ for $\delta^{18}O$, ± 0.05‰ for $\delta^{13}C$). For selected past time intervals, epibenthic $\delta^{13}C$ and $\delta^{18}O$ values were averaged for each of the investigated sites. Isotope values interpreted as brine water influenced were not included into the average.

Epibenthic $\delta^{18}O$ values were adjusted to $\delta^{18}O$ values of *Uvigerina peregrina* by adding 0.64‰ and used as proxy for bottom water density, assuming that sea bottom temperature at the LGM was close to the freezing point and the temperature effect on $\delta^{18}O$ changes can thus be ignored. Epibenthic $\delta^{13}C$ values, in turn, were used as proxy for bottom water ventilation (Duplessy 1982; Zahn *et al.* 1986; Curry *et al.* 1988). $\delta^{13}C$ signals of the three epibenthic *Cibicidoides* / *Cibicides* species outlined above are regarded as equally suitable for reconstructing the nutrient content of bottom water masses, as shown for *C. wuellerstorfi* and *C. lobatulus* by Weinelt *et al.* (2001). Voelker (1999) demonstrated by multiple analyses of single specimens of *C. lobatulus* and *C. pachyderma* that $\delta^{13}C$ values of these two species don't show any offset. On the other hand, Mackensen & Licari (2004) reported on $\delta^{13}C$ of "living" *C. wuellerstorfi* from the South Atlantic, that exceeds the values of "living" *C. pachyderma* and *C. lobatulus* by 0.2 to 0.6‰. The $\delta^{13}C$ values measured in cores to the north to the Denmark Strait are derived from *C. pachyderma* and *C. lobatulus* only, whereas the values from the Irminger Basin to the south are based on *C. wuellerstorfi* only. Accordingly, the glacial $\delta^{13}C$ values reconstructed for the Blosseville Basin in the north may be underestimated by 0.3‰.

We did not apply the +0.32‰ correction to glacial $\delta^{13}C$ values because they would exceed the maximum $\delta^{13}C$ value of 2‰ resulting from physical fractionation at the atmosphere-ocean interface. Spatial density gradients and the patterns of bottom water ventilation were plotted on vertical palaeoceanographic sections similar to those in Zahn *et al.* (1987). For this purpose, LGM stable-isotope values from each coring site were horizontally projected onto virtual vertical planes crossing the study area from north-east to south-west and west to east assuming horizontal water mass stratification, that is ignoring the asymmetries due to Coriolis forcing.

2.3 Age control

Chronology of core 15-3 is based on both magnetic and $\delta^{18}O$ stratigraphy. Correlation of relative magnetic palaeointensity and inclination with the North Atlantic reference record NAPIS 75 (Laj *et al.* 2000) form the framework for long-term age control for the last 75 kyr. The Norwegian Basin (65 kyr), Laschamp (41 kyr), and Mono Lake (34.5 kyr) events of minimum palaeointensity were identified as major correlation markers. This magneto-stratigraphic framework formed the basis for a stratigraphic correlation of the planktic $\delta^{18}O$ record of Site 15-3 with the high-resolution planktic $\delta^{18}O$ record of neighbour core 2644 (Millo *et al.* in press). The latter record has a robust chronology based on densely spaced ^{14}C datings and on tuning of the planktic $\delta^{18}O$ record to the incremental time scale of the GISP2 ice core (Voelker *et al.* 1998; Voelker *et al.* 2000). Age models of cores 3-2 and 4-3 are based on correlation of epibenthic $\delta^{18}O$ records with the ^{14}C-dated epibenthic $\delta^{18}O$ record of neighbour core 90-24 (Elliot *et al.* 1998; Elliot *et al.* 2002). The sediment record of core 4-3 does not reach the LGM but ends at the beginning of Marine Isotope Stage 2 (Fig. 4).

Correlation amongst the various $\delta^{18}O$ records was established using the software AnalySeries, version 1.2 (Paillard *et al.* 1996). In summary, planktic $\delta^{18}O$ record of core 15-3 correlates with those of 2644 with a squared correlation coefficient $r^2 = 0.40$, whereas $r^2 = 0.56 / 0.58$ for the correlation between benthic $\delta^{18}O$ records of cores 3-2 and 4-3 versus 90-24. Discrepancies are mainly due to still inadequate sampling resolution of core 15-3 and the lack of benthic foraminifera specimens in various sections of cores 3-2 and 4-3.

The age control of core 23519 is based on $\delta^{18}O$ stratigraphy, refined by five ^{14}C datings for the interval spanning the LGM, Heinrich event I (H1), and

Termination IA and IB. For reasons of internal consistency we converted ^{14}C dates older than 13 000 years into calibrated ages after Voelker *et al.* (1998) after deducing a global reservoir age of – 400 years. We are aware that in the North Atlantic region the reservoir effect near the end of H1 (15 kyr BP) as well as near the end of the Younger Dryas cold spell (approximately 11.6 kyr BP) was significantly higher than 400 years (Waelbroeck *et al.* 2001). This implies that the timing of H1 may be overestimated in our age models by up to 1.5 kyr. We followed the definition of the LGM time slice given by GLAMAP 2000 (Sarnthein *et al.* 2003). This definition relies on the assumption that foraminiferal $\delta^{18}O$ maxima in the North Atlantic Ocean correspond to the maximum extent of global ice sheets.

2.4 Results

Epibenthic $\delta^{18}O$ record for the LGM and H1

In our study region the benthic $\delta^{18}O$ values reach fairly constant maxima of 5.20 to 5.55‰ during the LGM (Fig. 3A, B). In addition, there are several episodes of significantly lighter $\delta^{18}O$ values which interrupt these plateaus. These events are particularly evident in the single-specimen benthic $\delta^{18}O$ records of cores 2644, 23519, and 15-3 where the isotope data reveal two distinct subgroups, one of them with a significant $\delta^{18}O$ offset toward lighter values (Fig. 3A, B). These abrupt benthic $\delta^{18}O$ excursions probably derived from short-term, possibly seasonal injections of high-density brine water as the result of sea-ice melt and formation in the surface ocean (Veum *et al.* 1992). These light values were excluded from the averages in Fig. 3.

During the LGM, the absolute benthic $\delta^{18}O$ signal culminates with values between 5.55 and 5.30‰ at the north-western Icelandic slope (2644) and values of 5.48 to 5.06‰ at Site 15-3 (Fig. 3A). At the southern entrance to the Denmark Strait Site 23519 shows benthic $\delta^{18}O$ values of 5.43 to 4.87‰ (Fig. 3B) whereas at the south-eastern Greenland slope $\delta^{18}O$ values span between 5.51 and 5.33‰ (Site 90-24, Elliot *et al.* 2002) (Fig. 4) and reach 5.35‰ at Site 3-2 (Fig. 3B). The onset of the meltwater regime of H1 was characterized by particularly distinct brine water spikes in the benthic $\delta^{18}O$ records at Sites 2644, 15-3, and 23519, signals that matched the abrupt meltwater-induced decrease in planktic $\delta^{18}O$ at the inception of H1 (Fig. 3A, B).

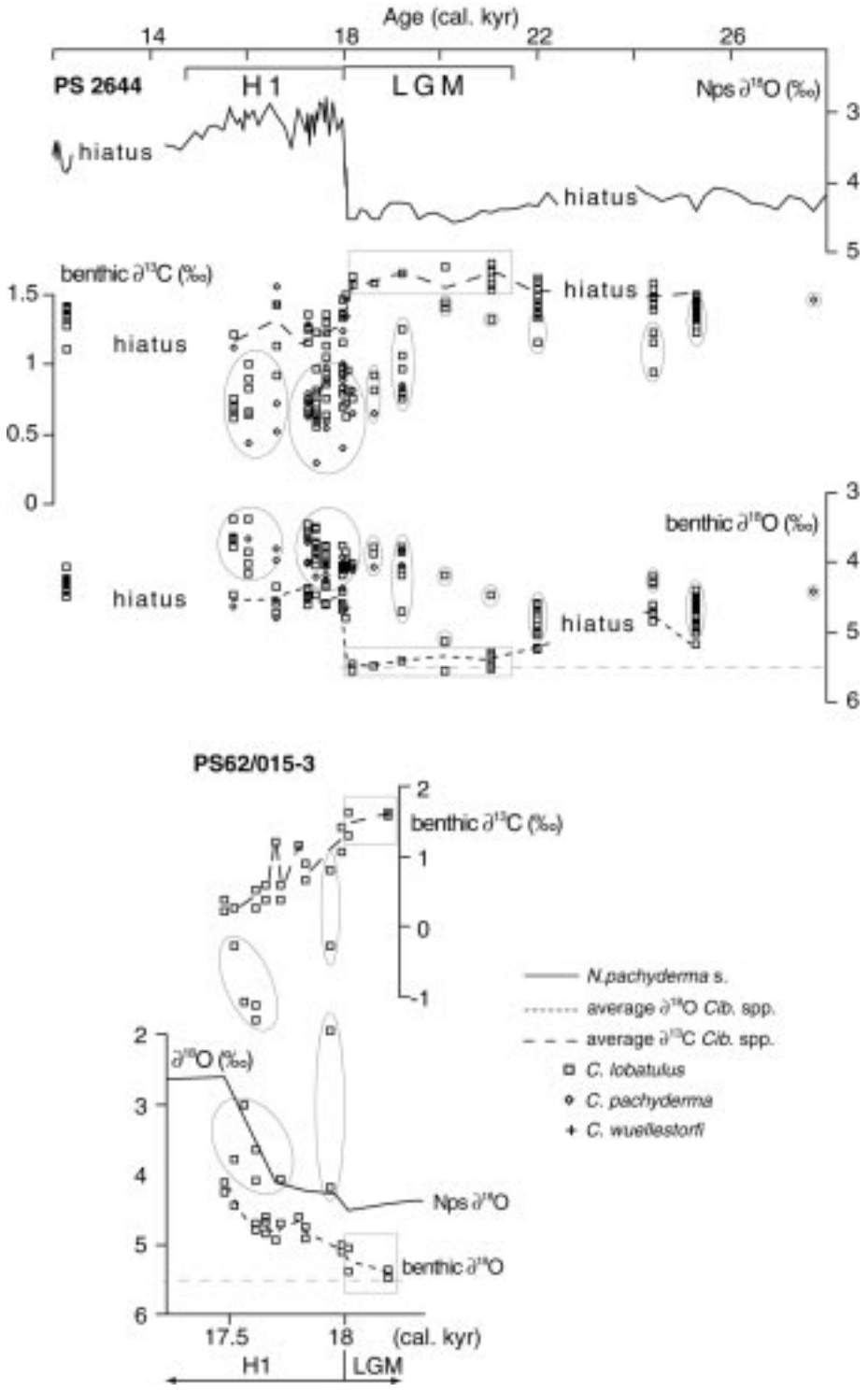

Fig. 3. (A) Single-specimen epibenthic $\delta^{13}C$ and $\delta^{18}O$ records of cores 2644 and 15-3 as compared to planktic (Nps) $\delta^{18}O$ record of core 2644 for stratigraphic reference. (B) Epibenthic $\delta^{13}C$ and $\delta^{18}O$ records of core 23519 (based on single-specimens) and 3-2 (multi-specimen record) as compared to Nps $\delta^{18}O$ record of core 2644. Circles enclose isotopic values obtained from foraminifera which probably have calcified their shell under the influence of isotopically light brine water. Dashed lines connect average isotopic values unbiased by brine water. Rectangles outline isotopic values selected for the reconstruction of the LGM water masses and density pattern in Fig. 7. Arrows indicate positions of ^{14}C datings (obtained from *N. pachyderma* s.).

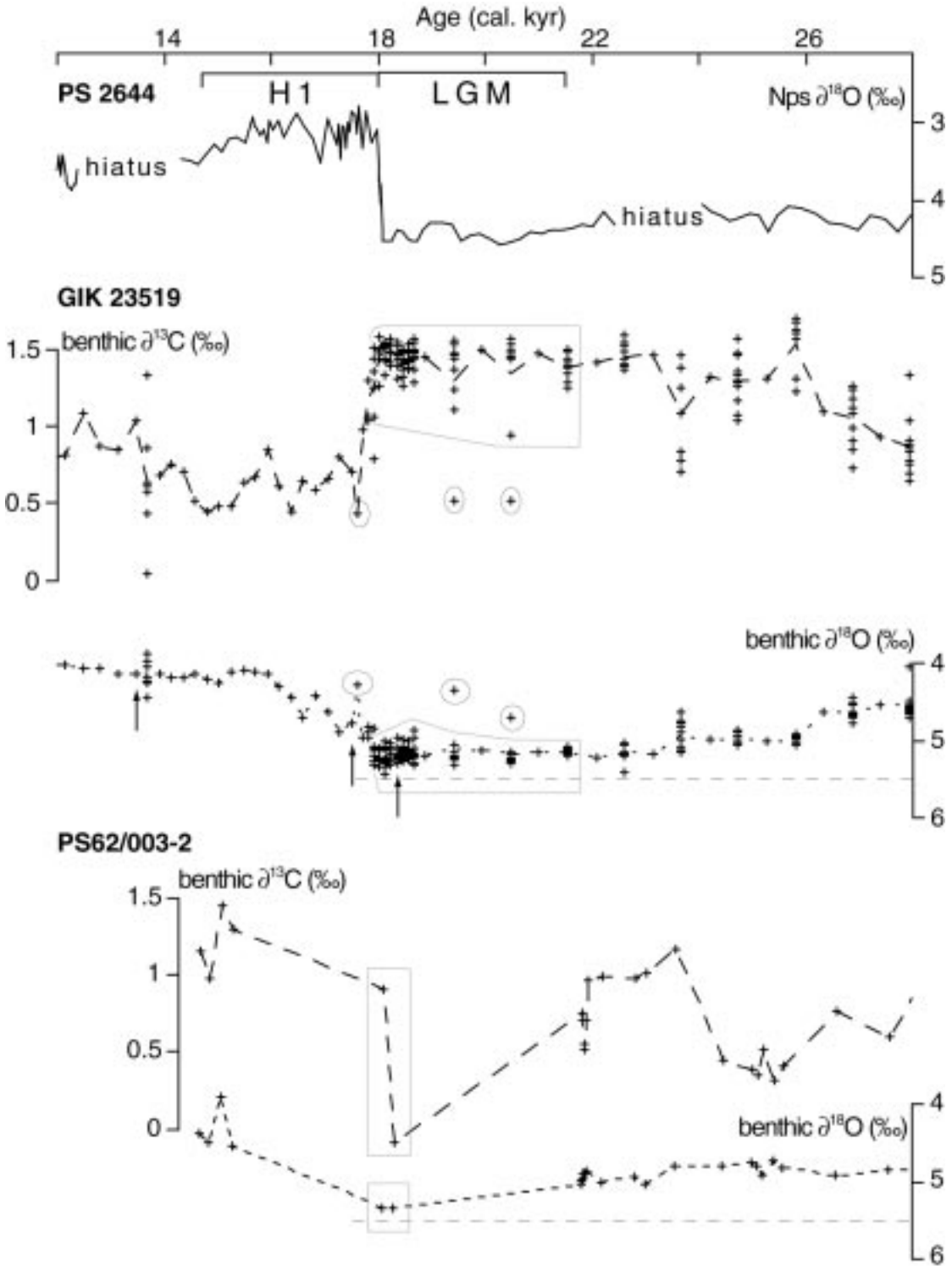

Fig. 3B (see previous page).

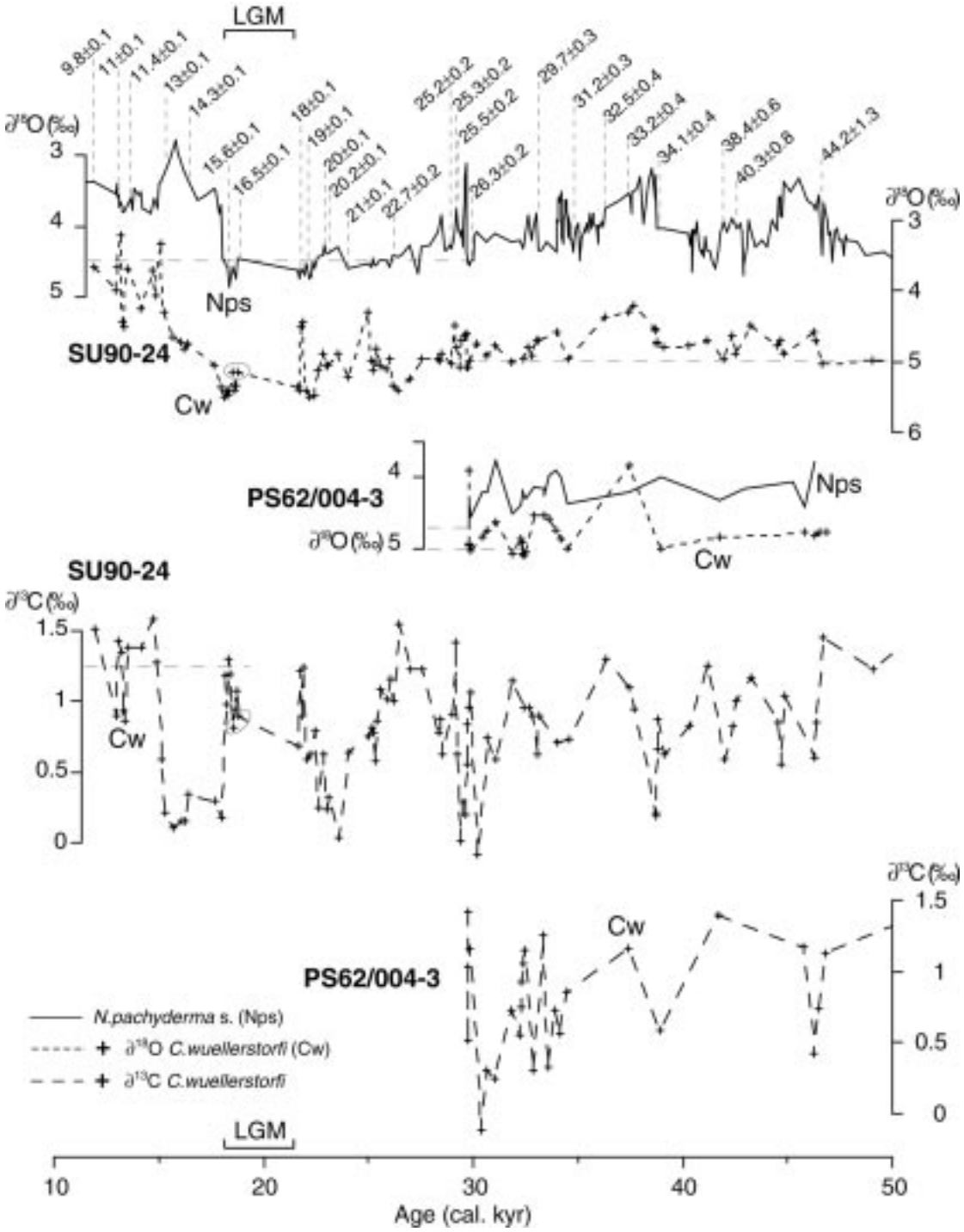

Fig. 4. Planktic $\delta^{18}O$ and multi-specimen epibenthic $\delta^{18}O$ and $\delta^{13}C$ records of core 90-24 (Elliot *et al.* 2002) and 4-3. Planktic $\delta^{18}O$ record and ^{14}C dates (in thousand years) of core 90-24 (Elliot *et al.* 2002) are displayed on top for stratigraphic reference. Planktic $\delta^{18}O$ record of core 4-3 is also plotted for comparison with those of 90-24. For explanation of symbols see Fig. 3.

Epibenthic $\delta^{13}C$ record for the LGM and H1

LGM epibenthic $\delta^{13}C$ values measured on single specimens vary by up to 1‰ within one and the same sample interval. Since low $\delta^{13}C$ values match low $\delta^{18}O$ values, it is likely that the ^{13}C-depletions were induced by brine water, as inferred for the coeval light $\delta^{18}O$ excursions (Fig. 3). After removing the brine water-induced light ^{13}C events, absolute $\delta^{13}C$ values reach 1.72 to 1.53‰ at Site 2644, the record of Site 15-3 exhibit values between 1.64 to 1.30‰ whereas they range between 1.58 to 1.06‰ at the southern outlet of the Denmark strait (23519) (Fig. 3A, B).

Absolute $\delta^{13}C$ values along the south-eastern Greenland slope, span between 1.30 and 0.18‰ at Site 90-24 (Elliot *et al.* 2002) (Fig. 4) and between 0.91 and –0.08‰ at Site 3-2 (Fig. 3B). Paucity of epibenthic foraminifera renders these records rather discontinuous, nonetheless they exhibit maximum and minimum values which may be highly indicative of changes in the palaeo-circulation patterns. Scarcity of epibenthic foraminifera may be attributed to low productivity and/or dilution of foraminiferal specimens in ice rafted detritus. In addition, microscope observations of highly dissolved epibenthic specimens of Sites 3-2 and 4-3 reveal that also dissolution reduced the availability of foraminifera.

At each location, the onset of H1 is accompanied by a drastic (probably abrupt) decrease of average benthic $\delta^{13}C$ values by approximately 0.5 to 1‰, which matches the planktic $\delta^{18}O$ meltwater signal and a reduction of epibenthic $\delta^{18}O$ by up to 1‰.

2.5 Discussion

A reconstruction of deepwater density gradients and bottom water ventilation is crucial to understand the variability of the DSO and its implications on the northern North Atlantic overturning during the LGM. On the basis of seismic, sub-bottom profiling, side-scan sonar, and sediment grain-sizes from the Southeast Greenland margin, Kuijpers *et al.* (2003) demonstrated that LGM bottom water circulation at about 1850 m water depth was reduced. These authors claim that the glacial DSO stopped repeatedly and had a significantly weaker flow regime than during the Holocene. On the other hand, summer sea surface temperatures of 3.5 to more than 4.0°C and extremely high planktic $\delta^{18}O$ values of 4.7 to 4.9‰ indicated that the glacial sea surface was ice-free over vast sea regions for a few summer months and that salinity in large areas of the Greenland-Iceland-Norwegian Seas was sufficiently

high for (short-term) seasonal deepwater convection (Weinelt *et al.* 1996; Sarnthein *et al.* 2003). In addition, benthic $\delta^{13}C$-based reconstructions of the spatial pattern of the LGM intermediate and deepwater ventilation in the Northern North Atlantic suggest that Glacial Upper North Atlantic Deepwater (GNADW) was formed or even enhanced to the south of Iceland at water depths similar to those of modern Labrador Sea Water (Jung 1996). In summary, one may expect that a minor DSO was active during the LGM, even though its flow direction might have been occasionally reversed. In addition, model experiments of Koesters *et al.* (2004) predict that the density contrast between north and south of the Denmark Strait was most probably reduced during the LGM and, accordingly, the path of the glacial DSO had shifted to shallower depths.

Duplessy *et al.* (2002) presented a global compilation of benthic $\delta^{18}O$ and $\delta^{13}C$ values for the LGM, showing that the heaviest $\delta^{13}C$ values have occurred in the North Atlantic, where they match maximum $\delta^{18}O$ values. This trend now is clearly prolonged to extremes of 5.55‰ $\delta^{18}O$ and 1.72‰ $\delta^{13}C$ by our single-specimen benthic stable-isotope records obtained from Sites 2644, 15-3, and 23519 (Fig. 5). If the $\delta^{13}C$ values of Sites 2644 and 15-3 are corrected for the offset outlined by Mackensen & Licari (2004), they will reach up to 2‰, that is the level of pure physical fractionation.

The glacial isotopic data make it possible to highlight the actual isotopic maxima, but also provide small-scale differential values within the range of a 1-cm thick sample (Figs 3A, B) as result of short-term variability (approximately 150 years). Such detailed information is averaged out by multi-specimen analyses, as revealed by comparing the LGM single-specimen benthic $\delta^{18}O$ record from Site 23519 with the multi-specimen benthic $\delta^{18}O$ record from the neighbouring Site 1225 (Fig. 6). Since LGM deepwater temperatures in our study area probably ranged close to the freezing point, the spatial distribution of epibenthic $\delta^{18}O$ primarily reflects a density pattern. Accordingly, the benthic oxygen and carbon isotope maxima of 5.55 and 1.72‰ at Site 2644 to the north of Iceland represent the densest and best ventilated deepwater in the global Ocean during the LGM (Fig. 5). This implies that the primary endmember source of LGM deepwater still was located in the Nordic Seas. At intermediate depths down to 1800 m, there was a clear north-south density

gradient from σ_0 of ~28.7 to 28.1, which clearly implies a DSO from north to south (Fig. 7E).

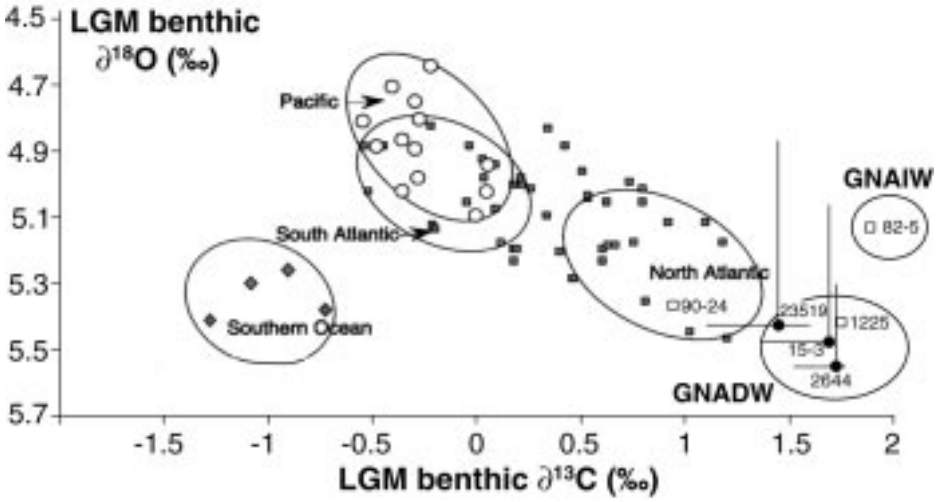

Fig. 5. Global compilation of $\delta^{18}O$ and $\delta^{13}C$ values of the epibenthic foraminiferal genus *Cibicides* for the LGM (Duplessy *et al.* 2002; supplemented). All $\delta^{18}O$ values have been corrected for vital-effect by adding 0.64‰. Diamonds = Southern Ocean; open circles = Pacific Ocean; closed squares = Atlantic Ocean; open squares = average values of cores 90-24 (Elliot *et al.* 2002), 1225 (Hagen & Hald 2002), and 82-5 (Jung 1996; van Kreveld *et al.* 2000). Vertical and horizontal bars show the total range of $\delta^{18}O$ and $\delta^{13}C$ values obtained from single-specimen isotope records of cores 23519, 15-3, and 2644. Full dots on the bar interception represent the $\delta^{18}O$ extremes matching $\delta^{13}C$ maxima, indicative of Glacial North Atlantic Deepwater (GNADW). Isotopic values at Site 82-5 represent Glacial North Atlantic Intermediate Water (GNAIW).

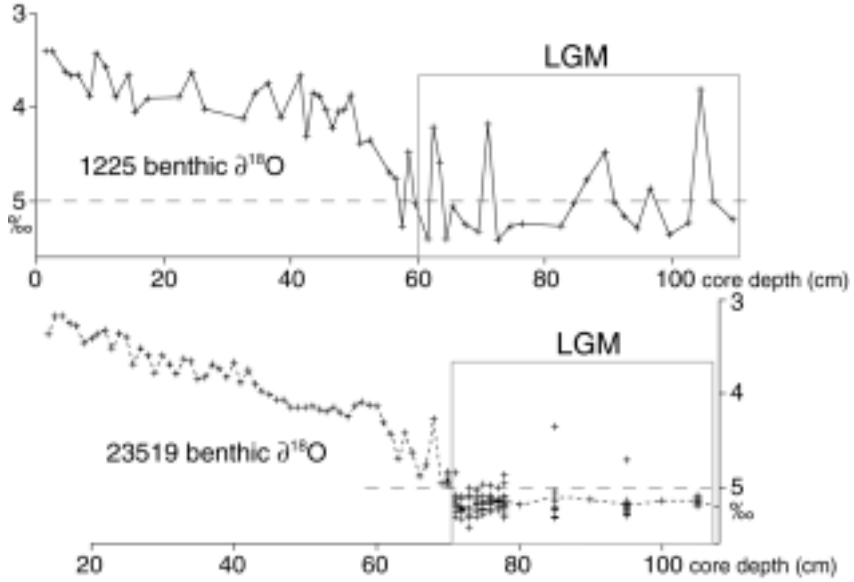

Fig. 6. Comparison of LGM epibenthic $\delta^{18}O$ record of Site 1225 (Hagen & Hald 2002) based on multi-specimen versus the record of neighbor Site 23519 based on single-specimen analyses. Both records are reported versus core depth. Single-specimen analyses highlight absolute maximum and minimum isotopic values and reveal more clearly the influence of brine water signals, which are largely averaged out by multi-specimen analyses.

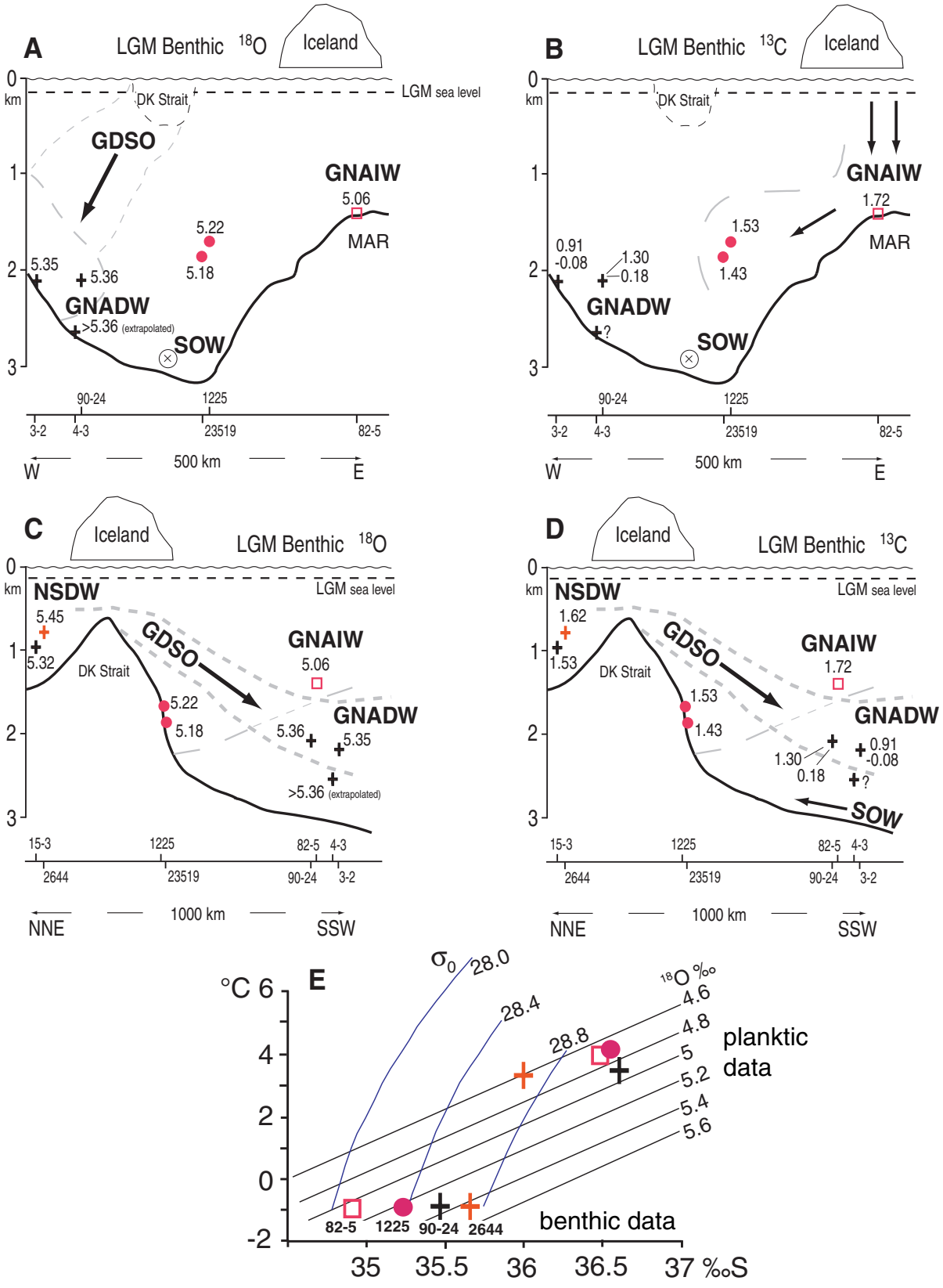

Fig. 7. Reconstruction of LGM water masses based on average LGM epibenthic ^{18}O (A and C) and ^{13}C values (B and D) obtained from the investigated sites after removing isotopic values biased by brine water. Stable-isotope values have been horizontally projected from each coring location onto virtual vertical planes crossing the study area from W to E (A and B) and NNE to SSW (C and D). Cores are indicated below the transects. Arrows indicate inferred paths of water masses. NSDW = Nordic Seas Deepwater, GDSO = Glacial Denmark Strait Overflow; GNAIW = Glacial North Atlantic Intermediate Water; GNADW = Glacial North Atlantic Deepwater; SOW = Southern Ocean Water; MAR = Mid Atlantic Ridge. (E) LGM epibenthic ^{18}O values obtained from sites to the north and south of the Denmark Strait plotted on a temperature-salinity-density (σ_0)- ^{18}O diagram (modified from Weinelt *et al.* 1996). Bottom water density at these locations is inferred assuming that LGM bottom water temperatures ranged close to the freezing point (approximately –1.6°C). LGM bottom water density at Site 2644 is nearly 0.6 denser than at Site 82-5. LGM planktic ^{18}O values obtained from the same sites are plotted for comparison in the upper part of the diagram.

Bottom water density slightly decrease to σ_0 of ~28.4 at the two sites close to the southern outlet of the Denmark Strait, with maximum $\delta^{18}O$ values of 5.43‰ and average values of 5.18‰ at Site 23519 and of 5.22‰ at nearby Site 1225 (Hagen & Hald 2002) (Fig. 7). In contrast, farther south, off south-east Greenland, epibenthic $\delta^{18}O$ values at Sites 90-24 and 3-2 reached a slightly higher maximum level of 5.51‰ and average $\delta^{18}O$ values to 5.36‰ (Figs 4, 7). At the deeper Site 4-3 $\delta^{18}O$ values greater than 5.36‰ may be assumed on the basis of stratigraphic and spatial extrapolations (Fig. 4). This pattern suggests that a glacial DSO-like deepwater incursion originated from dense and maximum ventilated water in the Nordic Seas and washed the eastern flank of the Greenland slope like today (Dickson & Brown 1994), eventually forming the GNADW (Fig. 7). On the other hand, relatively lower bottom water density inferred for Sites 23519 and 1225 indicates that the DSO has bypassed those locations to the west, higher upslope (Fig. 7), as predicted by the model of Koesters *et al.* (2004).

Epibenthic $\delta^{18}O$ values of 5.06‰ at Site 82-5 document a much reduced density (σ_0 ~28.1) on top of the Mid Atlantic Ridge (1417 m), where fairly constant $\delta^{13}C$ values of 1.72‰ document a maximum in bottom water ventilation throughout the LGM (Jung 1996; van Kreveld *et al.* 2000). This extreme competes with the previously outlined ventilation peak at Site 2644 in the Blosseville Basin with a maximum $\delta^{13}C$ value of 1.72‰ (Fig. 3A) and an average of 1.62‰ (Fig. 7). At greater depths, Blosseville Basin Site 15-3 exhibits a slightly lower ventilation with $\delta^{13}C$ values reaching up to 1.64‰ and an average of 1.53‰. Likewise, the records immediately to the south of the Denmark Strait are characterized by fairly high ventilation with average LGM values of 1.43 to 1.53‰ (Fig. 7) and single peaks of 1.73‰ at Site 1225 (Hagen & Hald 2002). In summary, there were two "competitive" separate LGM convection cells: One of them was located to the south of Iceland (Duplessy *et al.* 1991; Sarnthein *et al.* 1994) forming Glacial North Atlantic Intermediate Water (GNAIW), while the second convection cell produced deepwater with a slightly higher density to the north of the Denmark Strait. The match between heavy epibenthic $\delta^{18}O$ and $\delta^{13}C$ values to the north of Iceland (Fig. 3A) demonstrates that at least short-term pulses of high-density and highly ventilated water were advected from the Nordic Seas through the Denmark Strait into the deep Atlantic during the LGM, that was a source for GNADW. In addition, a number of distinct

events of light $\delta^{18}O$ and light $\delta^{13}C$ are documented in our single-specimen records, which suggest that seasonal plumes of brine water were an additional factor contributing to the formation of deep and intermediate water both to the north and the south of the Denmark Strait throughout the LGM (Fig 3A, B).

In addition, several incursions of strongly ^{13}C-depleted Southern Ocean Water are documented at the lowermost southeastern Greenland slope by absolute $\delta^{13}C$ minima of 0.18 and –0.08‰ at Sites 90-24 and 3-2 (Figs 3B, 4, 7). On the other hand, $\delta^{13}C$ maxima of 1.30 and 0.91‰ at these sites possibly reveal competition between the southern-source water mass and GNADW.

A pattern of deep and intermediate-water circulation totally different from the LGM is found for the subsequent meltwater regime of H1. A significant decrease in bottom water ventilation matches distinct brine-induced light $\delta^{18}O$ pulses in our benthic records starting from the onset of H1 (Fig. 3). These features point to a breakdown in the meridional overturn both to the north and south of the Denmark Strait and suggest a complete shut-off or reversal (south-north direction) of the DSO. Benthic bottom water temperature records may provide crucial evidence for past current directions.

2.6 Conclusions

A stable-isotope-based reconstruction of the bottom and intermediate water density pattern across the Denmark Strait over the LGM indicates a north-south density gradient from σ_0 ~28.7 to 28.1 at about 800 - 1800 m water depth. Maximum-density and highly ventilated water masses were convected to the north of the Denmark Strait and formed a southward flowing DSO and further downstream, the primary source of GNADW, flowing southward along the lower East Greenland slope like today.

To the south of Iceland highly ventilated but less dense GNAIW formed on top of the Mid Atlantic Ridge, in areas largely free of sea ice during both LGM summers and winters. During seasonal sea ice formation, plumes of high-density brine water were an additional factor that contributed to glacial deep and intermediate water formation both to the north and south of the Denmark Strait and dominated the scenario during subsequent H1 stadial.

Acknowledgements.- We are grateful to P. Grootes for ^{14}C datings and interesting discussions. Special thanks go to M. Weinelt for comments on density reconstructions. We acknowledge K. Kissling, D. Gudehus, N. Gehre, P. Springer, D. Magens, D. Petereit, R. Isemer, A. Klug, and M. Remetin for helping in sample preparation. We thank C. Sieler for data managing. The work was founded by the Deutsche Forschungsgemeinschaft (Kiel Forschergruppe 451).

References

Boyle, E.A. 1992: Cadmium and $\delta^{13}C$ paleochemical ocean distributions during the stage 2 glacial maximum. *Annual Reviews Earth Planetary Science 20,* 245-287.

Clark, P.U. & Mix, A.C. 2002: Ice sheets and sea level of the Last Glacial Maximum. *Quaternary Science Reviews 21*, 1-7.

CLIMAP Project Members (CLIMAP) 1981: Seasonal reconstructions of the Earth's surface at the Last Glacial Maximum, Map Chart Ser. MC-36. Geological Society of America, Boulder, Colorado.

Curry, W.B., Duplessy, J.C., Labeyrie, L.D. & Shackleton, N.J. 1988: Changes in the distribution of $\delta^{13}C$ of deep water ΣCO_2 between the last glaciation and the Holocene. *Paleoceanography 3*, 317-341.

Dickson, R.R. & Brown, J. 1994: The Production of North Atlantic Deep Water – Sources, Rates and Pathways. *Journal of Geophysical Research C99*, 12319-12341.

Dickson, R.R., Lazier, J., Meincke, J., Rhines, P. & Swift, J. 1997: Long-term coordinated changes in the convective activity of the North Atlantic. *Progress in Oceanography 38,* 241-295.

Dickson, B., Yashayaev, I., Meincke, J., Turrell, B., Dye, S. & Holfort, J. 2002: Rapid freshening of the deep North Atlantic Ocean over the past four decades. *Nature 416*, 832-837.

Dokken, T.M. & Jansen, E. 1999: Rapid changes in the mechanism of ocean convection during the last glacial cycle. *Nature 401*, 458-461.

Dörscher, R. & Redler, R. 1997: The relative importance of northern overflow and subpolar deep convection for the North Atlantic thermohaline circulation. *Journal of Physical Oceanography 27*, 1894-1902.

Duplessy, J.-C. 1982: North Atlantic Deep Water circulation during the last climatic cycle. *Bulletin Institut de Geólogie de Bassin d'Aquitaine 31*, 379-391.

Duplessy, J.-C., Labeyrie, L., Juillet-Leclerc, A., Maitre, F., Duprat, J. & Sarnthein, M. 1991: Surface salinity reconstruction of the North Atlantic Ocean during the LGM. *Oceanologica Acta 14,* 311-324.

Duplessy, J.-C., Labeyrie, L. & Waelbroeck, C. 2002: Constraints on the ocean oxygen isotopic enrichment between the Last Glacial Maximum and the Holocene: Paleoceanographic implications. *Quaternary Science Reviews 21*, 315-330.

Duplessy, J.-C., Shackleton, N.J., Fairbanks, R.G., Labeyrie, L., Oppo, D. & Kallel, N. 1988: Deepwater source variations during the last climatic cicle and their impact on the global deepwater circulation. *Paleoceanography 3*, 343-360.

Elliot, M., Labeyrie, L., Bond, G., Cortijo, E., Turon, J.L., Tisnerat, N. & Duplessy, J.-C. 1998: Millenial-scale iceberg discharges in the Irminger Basin during the last glacial period: Relationship with the Heinrich events and environmental settings. *Paleoceanography 13*, 433-466.

Elliot, M., Labeyrie, L. & Duplessy, J.-C. 2002: Changes in North Atlantic deep-water formation associated with the Dansgaard-Oeschger temperature oscillations (60-10 ka). *Quaternary Science Reviews 21*, 1153-1165.

Fleming, K. & Lambeck, K. 2004: Constraints on the Greenland Ice Sheet since the Last Glacial Maximum from sea-level observations and glacial-rebound models. *Quaternary Science Reviews 23*, 1053-1077.

Ganopolski, A., Rahmstorf, S., Petoukhov, V. & Claussen, M. 1998: Simulation of modern and glacial climates with a coupled global model of intermediate complexity. *Nature 391*, 351-356.

Gerdes, R. & Köberle, C. 1995: On the influence of DSOW in a numerical model of the North Atlantic general circulation. *Journal of Physical Oceanography 25,* 2624-2642.

Hagen, S. & Hald, M. 2002: Variation in surface and deep water circulation in the Denmark Strait, North Atlantic, during marine isotope stages 3 and 2. *Paleoceanography 17*, 1-16.

Hansen, B. & Østerhus, S. 2000: North Atlantic-Nordic Seas exchanges. *Progress in Oceanography 45*, 109-208.

Hansen, B., Turell, W.R. & Østerhus, S. 2001: Decreasing overflow from the Nordic Seas into the Atlantic Ocean through the Faeroe-Shetland Channel since 1950. *Nature 411*, 927-930.

Hewitt, C.D., Stouffer, R.J., Broccoli, A.J., Mitchell, J.F.B. & Valdes, P.J. 2003: The effect of ocean dynamics in a coupled GCM simulation of the Last Glacial Maximum. *Climate Dynamics 20,* 203-218.

Joussaume S. & Taylor, K.E. 2000: Proceedings of the third Paleoclimate Modeling Intercomparison Project (PMIP) workshop, edited by P. Braconnot, 271 pp.

Jung, S. 1996: Wassermassenaustausch zwischen NE-Atlantik und Nordmeer während der letzen 300,000/ 80,000 Jahre im Abbild stabiler O- und C-Isotope. *Berichte aus dem Sonderforschungsbereich 313 nr. 61*, University of Kiel, 104 pp.

Kim, S.J., Flato, G.M. & Boer, G.J. 2003: A coupled climate model simulation of the Last Glacial Maximum, Part 2: approach to equilibrium. *Climate Dynamics 20*, 635-661.

Kitoh, A., Murakami, S. & Koide, H. 2001: A simulation of the Last Glacial Maximum with a coupled atmosphere-ocean GCM. *Geophysical Research Letters 28,* 2221-2224.

Koesters, F., Kaese, R., Fleming, K. & Wolf, D. 2004: Denmark Strait overflow for Last Glacial maximum to Holocene conditions. *Paleoceanography 19 (2)*, PA2019.

van Kreveld, S., Sarnthein, M., Erlenkeuser, H., Grootes, P., Jung, S., Nadeau, M.J., Pflaumann, U. & Voelker, A. 2000: Potential links between surging ice sheets, circulation changes, and the Dansgaard-Oeschger cycles in the Irminger Sea, 60-18 kyr. *Paleoceanography 15*, 425-442.

Kuijpers, A., Troelstra, S.R., Prins, M.A., Linthout, K., Akhmetzhanov, A., Bouryak, S., Bachmann, M.F., Lassen, S., Rasmussen, S. & Jensen, J.B. 2003: Late Quaternary sedimentary processes and ocean circulation changes at the Southeast Greenland margin. *Marine Geology 195*, 109-129.

Laj, C., Kissel, C., Mazaud, A.,Channell, J.E.T. & Beer, J. 2000: North Atlantic paleointensity stack since 75 ka of the Laschamp event. *Royal Society of London Philosophical Transactions A 358*, 1009-1025.

Lambeck, K. & Chappell, J. 2001: Sea level change through the last glacial cycle. *Science 292*, 679-686.

Larsen, B. 1983: Geology of the Greenland-Iceland Ridge in the Denmark Strait. *In* Bott, M.H.P., Saxov, S., Talwani, M. & Thiede, J. (eds.): *Structure and Development of the Greenland-Scotland Ridge: New Methods and Concepts*, 425-444. Plenum Press, New York.

Mackensen, A. & Licari, L. 2004: Carbon isotopes of live benthic foraminifera from the South Atlantic: Sensitivity to bottom water carbonate saturation state and organic matter rain rates. *In* Wefer, G., Mulitza, S. & Ratmeyer, V. (eds.): *The South Atlantic in the late Quaternary: Reconstruction of material budgets and current systems*, 623-644. Springer, Berlin.

McManus, J.F., Francois, R., Gheradi, J.M., Keigwin, L.D. & Brown-Leger, S. 2004: Collapse and rapid resumption of Atlantic meridional circulation linked to deglacial climate changes. *Nature 428*, 834-837.

Nørgaard-Pedersen, N., Spielhagen, R.F., Erlenkeuser, H., Grootes, P.M., Heinemeier, J. & Knies, J. 2003: Arctic Ocean during the Last Glacial Maximum: Atlantic and polar domains of surface water mass distribution and ice cover. *Paleoceanography 18 (3)*, 8.

Paillard, D., Labeyrie, L. & Yiou, P. 1996: Macintosh program performs time-series analysis. *EOS Transactions American Geophysical Union 77*, p. 379.

Paul, A. & Schäfer-Neth, C. 2003: Modeling the water masses of the Atlantic Ocean at the last Glacial Maximum. *Paleoceanography 18 (3)*, 3.

Peltier, W.R. 1994: Ice age paleotopography. *Science 265*, 195-201.

Prange, M., Romanova, V. & Lohmann, G. 2002: The glacial thermohaline circulation: Stable or unstable ? *Geophysical Research Letters 29 (21),* 24.

Sarnthein, M., Pflaumann, U. & Weinelt, M. 2003: Past extent of sea ice in the northern North Atlantic inferred from foraminiferal paleotemperature estimates. *Paleoceanography 18*, 1-8.

Sarnthein, M., Winn, K., Jung, S.J.A., Duplessy, J.-C., Labeyrie, L., Erlenkeuser, H. & Ganssen, G. 1994: Changes in east Atlantic deepwater circulation over the last 30,000 years: Eight time slice reconstructions. *Paleoceanography 9,* 209-267.

Schmittner, A., Meissner, K.J., Eby, M. & Weaver, A.J. 2002: Forcing of the deep ocean circulation in simulations of the last glacial maximum. *Paleoceanography 17 (2)*, 5.

Skinner, L.C. & Shackleton, N.J. 2004: Rapid transient changes in the northeast Atlantic deep water ventilation age across termination I. *Paleoceanography 19 (2)*, PA 2005.

Veum, T., Jansen, E., Arnoldt, M., Beyer, I. & Duplessy, J.-C. 1992: Water mass exchange between the North Atlantic and the Norwegian Sea during the past 28.000 years. *Nature 356*, 783-785.

Voelker, A.H. 1999: *Zur Deutung der Dansgaard-Oeschger Ereignisse in ultra-hochauflösenden Sedimentprofilen aus dem Europäischen Nordmeer.* Ph.D. dissertation, University of Kiel, 180 pp.

Voelker, A. H., Grootes, P.M., Nadeau, M.-J. & Sarnthein, M. 2000: Radiocarbon levels in the Iceland Sea from 25-53 ka and their link to the Earth's Magnetic Field Intensity. *Radiocarbon 42*, 437-452.

Voelker, A. H., Sarnthein, M., Grootes, P.M., Erlenkeuser, H., Laj, C., Mazaud, A., Nadeau, M. J. & Schleicher, M. 1998: Correlation of marine ^{14}C ages from the Nordic Seas with the GISP2 isotope record: implications for ^{14}C calibration beyond 25 ka BP. *Radiocarbon 40*, 517-534.

Waelbroeck, C., Duplessy, J.C., Michel, E., Labeyrie, L., Paillard, D. & Duprat, J. 2001: The timing of the last deglaciation in North Atlantic climate records. *Nature 412*, 724-726.

Weinelt, M., Kuhnt, W., Sarnthein, M., Altenbach, A., Costello, O., Erlenkeuser, H., Pflaumann, U., Simstich, J., Struck, U., Thies, A., Trauth, M.H. & Vogelsang, E. 2001: Paleoceanographic proxies in the northern North Atlantic. *In* Schäfer, P., Ritzrau, W., Schlüter, M. & Thiede, J. (eds.): *The northern North Atlantic: A changing environment*, 319-352. Springer, Berlin.

Weinelt, M., Sarnthein, M., Pflaumann, U., Schulz, H., Jung, S. & Erlenkeuser, H. 1996: Ice-free Nordic Seas during the Last Glacial Maximum? Potential sites of deepwater formation. *Paleoclimate 1,* 283-309.

Whitehead, J.A., Leetmaa, A. & Knox, R.A. 1974: Rotating hydraulics of strait and sill flows. *Geophysical Fluid Dynamics 6*, 101-125.

Yu, E.-F., Francois, R. & Bacon, M.P. 1996: Similar rates of modern and last-glacial ocean thermohaline circulation inferred from radiochemical data. *Nature 379*, 689-694.

Zahn, R., Sarnthein, M. & Erlenkeuser, H. 1987: Benthos isotopic evidence for changes of the Mediterranean outflow during the late Quaternary. *Paleoceanography 2*, 543-559.

Zahn, R., Winn, K. & Sarnthein, M. 1986: Benthic foraminiferal $\delta^{13}C$ and accumulation rates of organic carbon: *Uvigerina peregrina* group and *Cibicidoides wuellerstorfi*. *Paleoceanography 1,* 27-42.

CHAPTER 3

Methane signals and variations in Denmark Strait Overflow

3A. Methane-driven Late Pleistocene $\partial^{13}C$ minima and Overflow reversals in the S.W. Greenland Sea

CHRISTIAN MILLO, MICHAEL SARNTHEIN, HELMUT ERLENKEUSER AND THOMAS FREDERICHS

Christian Millo (cm@gpi.uni-kiel.de) and Michael Sarnthein, Department of Geology, Christian-Albrechts-Universitaet, Olshausenstrasse 40, D-24118 Kiel, Germany;

Helmut Erlenkeuser, Leibniz-Labor for Radiometric Dating and Isotope Research, Max-Eyth-Strasse 11, D-24118 Kiel, Germany;

Thomas Frederichs, Department of Geology, University of Bremen, Klagenfurter Strasse, D-28359 Bremen, Germany.

Accepted for publication in *Geology* on 6 July 2005.

ABSTRACT

A core transect across the southwestern Greenland Sea reveals coeval events of extremely negative planktic and benthic $\delta^{13}C$ excursions between 40 and 87 ka. The most pronounced event, Event 1, began at peak Dansgaard-Oeschger (DO) stadial 22 (85 ka) with a duration of 18 k.y. During this episode, incursions of Atlantic Intermediate Water caused a bottom water warming of up to 8 °C. Amplitude, timing, and geographic pattern of the $\delta^{13}C$ events suggest that this bottom water warming triggered clathrate instability along the East Greenland slope and a methane-induced depletion of $\delta^{13}C_{DIC}$ (DIC—dissolved inorganic carbon). Since $\delta^{13}C$ Event 1 matches a major peak in atmospheric CH_4 concentration (Blunier and Brook, 2001), this clathrate destabilization may have contributed to the rise in atmospheric CH_4 and thus to climate warming over marine isotope stage (MIS) 5.1.

Keywords: Clathrates, global warming, Denmark Strait Overflow, Heinrich events.

3A.1 INTRODUCTION

Striking planktic and benthic ^{13}C depletions up to –7‰ in several Quaternary isotope records have been interpreted as evidence for thermal destabilization of methane hydrates linked to episodes of bottom water warming, and it has also been suggested that clathrate instability may have driven abrupt decreases in $\delta^{13}C$ of oceanic dissolved inorganic carbon ($\delta^{13}C_{DIC}$) (Kennett et al., 2000; de Garidel-Thoron et al., 2004; Hill et al., 2004a). Since many negative $\delta^{13}C$ events match peaks in atmospheric CH_4, it has been proposed that CH_4 released at the seafloor escaped into the atmosphere and contributed to climate warming (Kennett et al., 2003), in addition to atmospheric CH_4 that originated from wetlands (Brook et al., 1999).

In this paper, we report on extreme planktic and benthic $\delta^{13}C$ minima in late Pleistocene sediment records from the southwestern Greenland Sea (Fig. 1). Since the most prominent $\delta^{13}C$ events occurred during times of potential advection of relatively warm intermediate water from the North Atlantic, we suggest that thermally induced clathrate destabilization and CH_4 release along the East Greenland margin may have driven regional changes in $\delta^{13}C_{DIC}$, in bottom and surface water, that can be traced across this margin, with likely CH_4 emissions into the atmosphere.

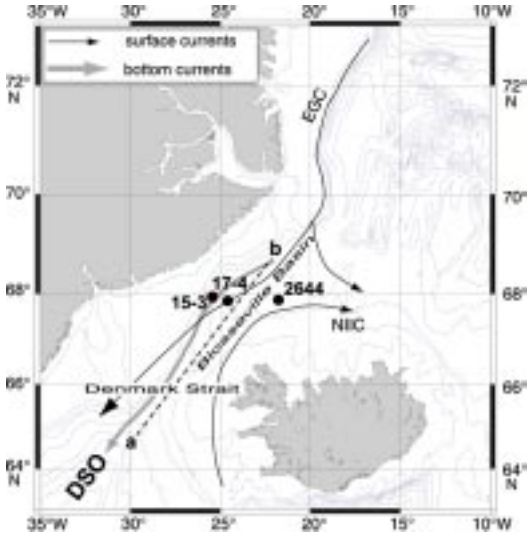

Figure 1. Core sites and surface and deep water currents in Blosseville Basin. EGC—East Greenland Current, NIIC—North Icelandic Irminger Current, DSO—Denmark Strait Overflow, a–b is position of paleoceanographic profile in Figure 5.

Previously, Smith et al. (2001) presented sediment records from the East Greenland shelf (400–600 m water depth), which documented three successive planktic and benthic $\delta^{13}C$ excursions to –7‰ between 14.0 and 9.3 cal (calendar) ka. Since the spatial and temporal patterns of these $\delta^{13}C$ events parallel the deglacial

retreat of ice sheets, the authors concluded that the $\delta^{13}C$ excursions were linked to dissociation of clathrate due to a reduction in ice load and intrusion of warm bottom water.

3A.2 STUDY AREA

Our sediment records were obtained from the Blosseville Basin to the north of the Denmark Strait, between East Greenland and northwest Iceland, with maximum water depths of 1500 m (Fig. 1). Along the northwestern basin margin, the East Greenland Current (EGC) carries cold and low-salinity water southward; along Iceland the northern branch of the Irminger Current carries warm and high-salinity water to the northeast. This water mass cools in winter, is convected, and in part forms the Denmark Strait Overflow (DSO), an important source of North Atlantic Deep Water.

Hemipelagic site Polarstern (PS) 62/015-3 (named site/core 15-3; 67°55.85′N, 25°25.59′W, 980 m water depth [mwd]) and clayey pelagic site PS 62/017-4 (named site/core 17-4; 67°51.01′N, 24°35.12′W, 1458 mwd) today are bathed in the DSO below extensive sea ice (and icebergs) characteristic of the East Greenland margin. Hemipelagic site PS 2644 (named site/core 2644; 67°52.02′N, 21°45.92′W, 777 mwd) is located below the northern branch of the Irminger Current (Fig. 1).

3A.3 METHODS

Core 15-3 was sampled every 5 cm from the core top down to 200 cm below sediment surface (bsf), every 2–3 cm from 200 to 400 cm bsf, and further below at each centimeter down to the core bottom (636 cm). In 17-4 (632 cm) sampling spaces were 1–2 cm. Samples were washed over a 63µm sieve and dried at 40 °C.

In both cores the concentration of foraminifera was highly variable, some intervals being barren. Up to 25 specimens of planktic *Neogloboquadrina pachyderma* sinistral (150–250 µm) and 1–10 specimens of epibenthic *Cibicides lobatulus* (250–400 µm) were picked for multiple- and single-specimen stable-isotope analysis, respectively. Isotopic data of core 2644 are from Voelker (1999).

Following standard preparation routines, foraminiferal samples were gently crushed, ultrasonically cleaned in ethanol, and dried. O and C stable isotopes were measured at the Leibniz Laboratory at Kiel University using the Kiel Carboprep line

and an automated MAT-251 mass spectrometer (analytical precision: ±0.07‰ for $\delta^{18}O$, ±0.05‰ for $\delta^{13}C$ PDB).

The preservation state of planktic and benthic foraminifera and their trace-element compositions were estimated from selected representative specimens using a scanning electron microscope (SEM) and energy dispersive x-ray (EDX) (CAMSCAN Serie 2 CS 44). SEM and EDX analyses of *C. lobatulus* were carried out on single test fragments, the remainder of tests were used for single-test stable-isotope analysis.

3A.4 AGE CONTROL

The chronology of cores 15-3 and 17-4 is based on both $\delta^{18}O$ and paleomagnetic stratigraphy. Primary age control for the last 75 k.y. was based on a correlation of relative magnetic paleointensity signals in cores 15-3 and 17-4 with the reference record NAPIS 75 (Laj et al., 2000), which employs the age control of core 2644 (Voelker et al., 1998) (Fig. 2A–C). Norwegian Basin (ca. 60–65 ka), Laschamp (41 ka), and Mono Lake (34.5 ka) events of minimum paleointensity form major correlation markers. In total, the various $\delta^{18}O$ and magnetic records correlate well for the core sections older than 30 ka. In addition, planktic $\delta^{18}O$ records of cores 15-3 and 17-4 were fine tuned to that of neighboring core 2644, which has a robust chronology based on numerous ^{14}C datings and on tuning to the incremental time scale of Greenland Ice Sheet Project 2 (GISP2) (Fig. 2D–F). Abrupt negative $\delta^{18}O$ excursions in core 2644 reflect meltwater pulses associated with Heinrich Events (HE) 1–6 and other cold Dansgaard-Oeschger (DO) stadials, since coeval planktic-foraminifera-based sea-surface temperature estimates do not reveal any significant warming (Voelker, 1999). The end of each meltwater spike is linked to an abrupt temperature increase over Greenland and in the northern North Atlantic (van Kreveld et al., 2000).

Because of internal consistency, we used the GISP2 time scale (Grootes and Stuiver, 1997) as stratigraphic base for marine isotope stages (MIS) 3 and 4. Sections older than 75 ka were dated by the scheme of North Greenland Ice Core Project (2004) members. The record of core 15-3 reaches back to 86.5 ka, the center of MIS 5.2, core 17-4 spans the last 78 k.y.

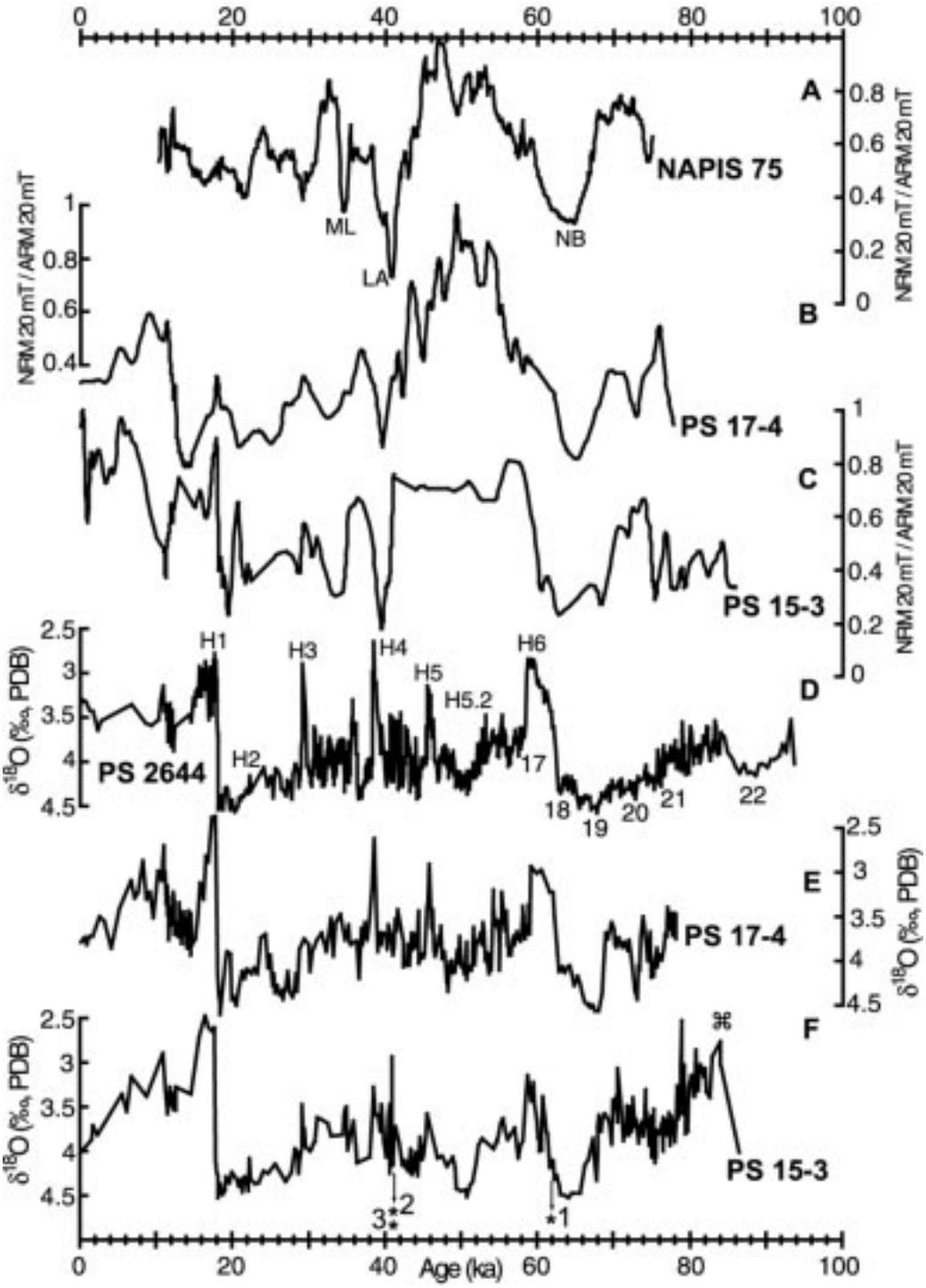

Figure 2. Correlation of North Atlantic paleointensity stack NAPIS 75 (including record of core PS2644; Laj et al., 2000) (A) versus relative magnetic paleointensity records (normalized to their respective means) of cores 17-4 (B) and 15-3 (C). Lower panel shows correlation of *N. pachyderma* $\delta^{18}O$ record of core 2644 (D) (Voelker, 1999) versus $\delta^{18}O$ records of cores 17-4 (E) and 15-3 (F) on Greenland Ice Sheet Project 2 (GISP2) time scale; NRM—Natural remanent magnetization; ARM—Anhysteretic remanent magnetization; PDB—Peedee belemnite. Asterisks mark positions of ^{14}C ages on *N. pachyderma* (corrected for ^{14}C reservoir effect of –400 yr); age 1 (KIA 24091) = >52 ka; ages 2 and 3 on *N. pachyderma* (KIA 24408) are 35.84 ka (using background ^{14}C level of marine isotope stage [MIS] 5 in core 2644) and 36.47 ka (using general pre-Eemian ^{14}C background), respectively. ⌘—Major meltwater event.

Correlations were carried out with the AnalySeries program (Paillard et al., 1996). The $\delta^{18}O$ squared correlation coefficients (r^2) reach 0.40 and 0.60 for the tuning of cores 15-3 and 17-4 to 2644, respectively. Discrepancies result from insufficient sampling resolution of cores 15-3 and 17-4.

3A.5 RESULTS

Outstanding ∂^{13}C minima:

Over the last 44 k.y. planktic $\delta^{13}C$ values at site 15-3 little deviate from 0.25‰. Further back there are two events of extreme ^{13}C depletion (Fig. 3).

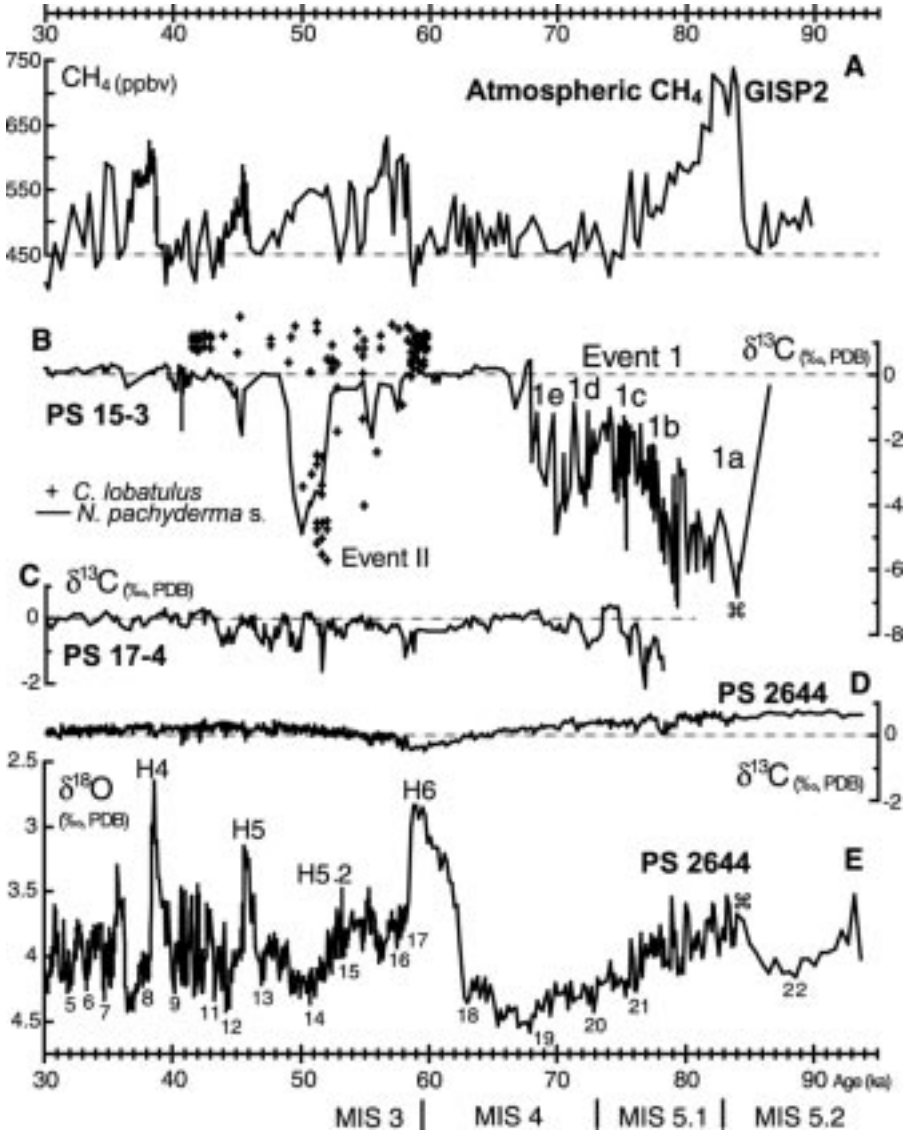

Figure 3. Greenland Ice Sheet Project 2 (GISP2) atmospheric CH_4 record (Blunier and Brook, 2001) (A) plotted versus planktic (*Neogloboquadrina pachyderma* sinistral) and benthic (*Cibicides lobatulus*) $\delta^{13}C$ minima (Events 1a to 1e, and II) in core 15-3 (B), and planktic $\delta^{13}C$ records of cores 17-4 (C) and 2644 (D). Planktic $\delta^{18}O$ record of core 2644 (E) serves for stratigraphic reference. Heinrich (H) events and Dansgaard-Oeschger (DO) interstadials are numbered. MIS—marine isotope stages; ⌘—time of major meltwater event (also see Fig. 2).

The most prominent Event 1a-1e started in the middle of MIS 5.2 (85 ka) and in total lasted for 18 k.y., including a broad scatter of values. The most negative $\delta^{13}C$ excursions (Event 1a) reached −7‰ during peak DO stadial 22 (84 ka) and subsequent to DO interstadial 21 (Event 1b; ca. 78 ka). The younger portion of Event 1 (c to e) correlates to DO stadial 20 (73 ka) and subsequent interstadial 19 (68 ka) and is marked by values of −1‰ to −4‰. Following 68 ka the $\delta^{13}C$ signal increased to the long-term average near 0‰. Event II, reaching –5‰, began at ~52 ka and lasted for 4 k.y., including the onset of DO interstadial 14 (51 ka). Minor pulses up to −2‰ occurred at 57.5 (DO interstadial 16), 55.5, 45.4 (end of H5; onset of DO interstadial 12), and 40.7 ka (near interstadial 9). Epibenthic $\delta^{13}C$ values closely parallel the extreme $\delta^{13}C$ excursion of Event II (no epibenthic foraminiferal tests were found at Event 1).

Core 17-4 also exhibited negative $\delta^{13}C$ excursions coeval with Events 1b and 1c in core 15-3 (Fig. 3), with –2.1‰ near 77 ka. Further up in the core, $\delta^{13}C$ values oscillate between 0‰ and –1‰, with a second prominent minimum of –1.6‰ at 51.5 ka, matching the onset of Event II in core 15-3. Accordingly, the $\delta^{13}C$ anomalies of Events 1 and II decrease eastward from the Greenland slope toward the central Blosseville Basin. Whereas the start of Events 1a and 1b is linked to meltwater regimes during MIS 5.1 and 5.2, the main pulse of Event II parallels early DO interstadial 14 and does not match a local meltwater pulse.

No negative $\delta^{13}C$ extremes mark the *N. pachyderma* record of core 2644, most distant from Greenland, just a steady slight $\delta^{13}C$ decrease toward the end of MIS 4.

Distribution of secondary crystalline overgrowth:

The test surface of several hundred planktic specimens and >100 benthic foraminiferal specimens in core 15-3 were studied using light microscopy in sections with and without negative $\delta^{13}C$ excursions. About 20 specimens were examined using SEM. Accordingly, ^{13}C-depleted intervals are dominated by altered specimens (and viceversa) (Fig. 4).

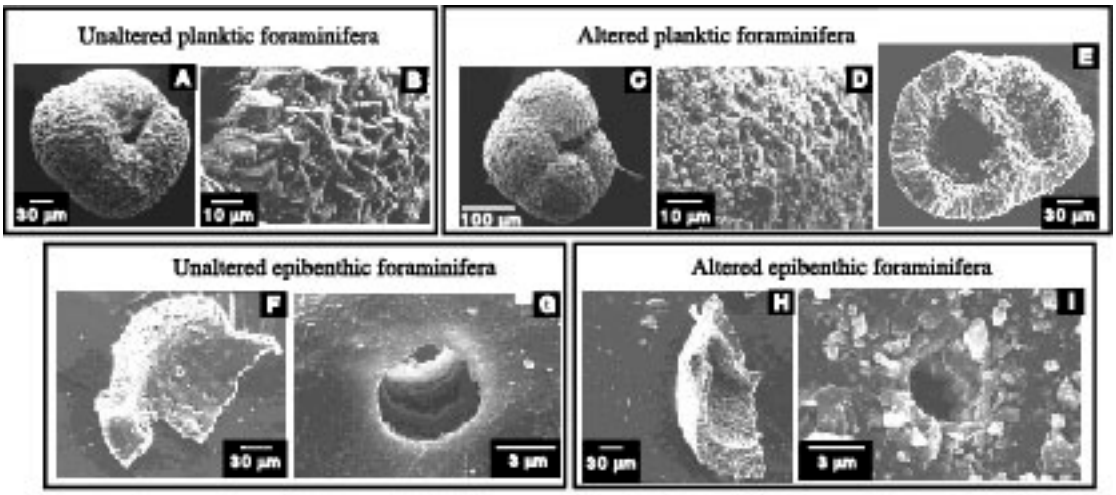

Figure 4. Scanning electron microscope (SEM) photographs of *Neogloboquadrina pachyderma* sinistral (A–E) and of fragments of *Cibicides lobatulus* (F–I). Pristine shell structure of tests with "normal" $\delta^{13}C$ values are shown in (B) and (G); details of overgrowth in ^{13}C-depleted tests are shown in (D) and (I). Inner wall side (E) of *N. pachyderma* s. overcrusted by needles of authigenic calcite.

Joint stable-isotope and SEM analyses on subsamples of *N. pachyderma* from 538 cm bsf (Event 1c), 418, 423 cm (Event II), and of *C. lobatulus* from 400 and 426 cm (Event II) showed that tests with negative $\delta^{13}C$ signatures were overcrusted by authigenic calcite (Fig. 4), whereas tests with nondepleted $\delta^{13}C$ values hardly showed this feature. Single-specimen $\delta^{13}C$ values of epibenthic *C. lobatulus* within one and the same sediment sample scattered more strongly in ^{13}C-depleted intervals (–5.5‰ to 1.5‰) than outside (Fig. 3).

Internal and external overgrowth of secondary calcite needles and cryptocrystals affected planktic, epibenthic, and endobenthic foraminifera (Fig. 4), being related to shell porosity rather than to the habitat. Planktic *N. pachyderma* specimens were most affected, followed by endobenthic *Melonis barleeanus* and *Cassidulina teretis*, and by epibenthic *C. lobatulus*.

No secondary overgrowths of calcite occurred on foraminifera in core 17-4.

Primary versus authigenic $\partial^{13}C$ signature:

SEM observations of *N. pachyderma* suggest that the inner and outer authigenic overgrowth totals up to 10%–20% of the total test, the remaining 90%–80% belong to the primary test (Fig. 4E). Assuming that primary and authigenic calcite may have a different response to dissolution, we leached two subsets of *N. pachyderma* obtained from Event II (423 cm bsf, 50.5 ka) in 1% HCl up to 30% and 60% of their original mass and attempted to quantify the potential influence of

authigenic calcite on $\delta^{13}C$ values. Stable-isotope analysis revealed a trend from pre-leaching $\delta^{13}C$ values of –4‰ to –5 ‰ to a (60%) post-leaching $\delta^{13}C$ value of –6.5‰, which appear to represent remnants of the primary shell ultrastructure, because the remainder of dissolved *N. pachyderma* tests revealed honeycomb structures under the SEM (J.P. Kennett, 2005; oral communication).

The isotope trend implies that the dissolved component (60%) must have a $\delta^{13}C$ value around –2.5‰ to –4‰. If the primary test has a homogeneous isotopic composition, the pre-leaching $\delta^{13}C$ values of –4‰ to –5‰ may result from mixing primary $CaCO_3$ (80%–90%, with $\delta^{13}C$ values of 0‰ to –4‰) with authigenic $CaCO_3$ (10%–20%, with $\delta^{13}C$ values as low as –9‰ to –50‰). In summary, both primary and authigenic carbonate are considered as ^{13}C depleted. The extremely low $\delta^{13}C$ values inferred for secondary overgrowth compare well with $\delta^{13}C$ values of authigenic carbonate found at sites with active hydrocarbon seepage (Eichhubl et al., 2000).

3A.6 DISCUSSION AND CONCLUSIONS

The outlined negative $\delta^{13}C$ excursions appear synchronous at two neighbor sites, with decreasing amplitudes from the East Greenland slope toward the east. Neither nutrient-poor surface and bottom water nor Quaternary sediments poor in ^{13}C-depleted organic matter (Schlueter et al., 2001) can account for the magnitude of the negative $\delta^{13}C$ anomalies recorded in these cores obtained below the EGC. Thus, we suggest that foraminifera incorporated isotopically light carbon released from methane hydrates during thermal destabilization and subsequent oxidation of CH_4 to the DIC pool in the overlying water column (Rathburn et al., 2003; Hill et al. 2004b).

The mega-$\delta^{13}C$ excursion of Event 1 occurred during MIS 5.2, a time of major meltwater discharge and minimum sea-surface salinity in the Arctic and Nordic Seas, as documented by coeval broad planktic $\delta^{18}O$ minima (Fig. 2D–F). We suggest that the low sea-surface salinity led to cessation of deep water convection, a reversal of the DSO, and northward incursion of relatively warm (up to 8 °C) upper Atlantic Intermediate Water (AIW; Fig. 5).

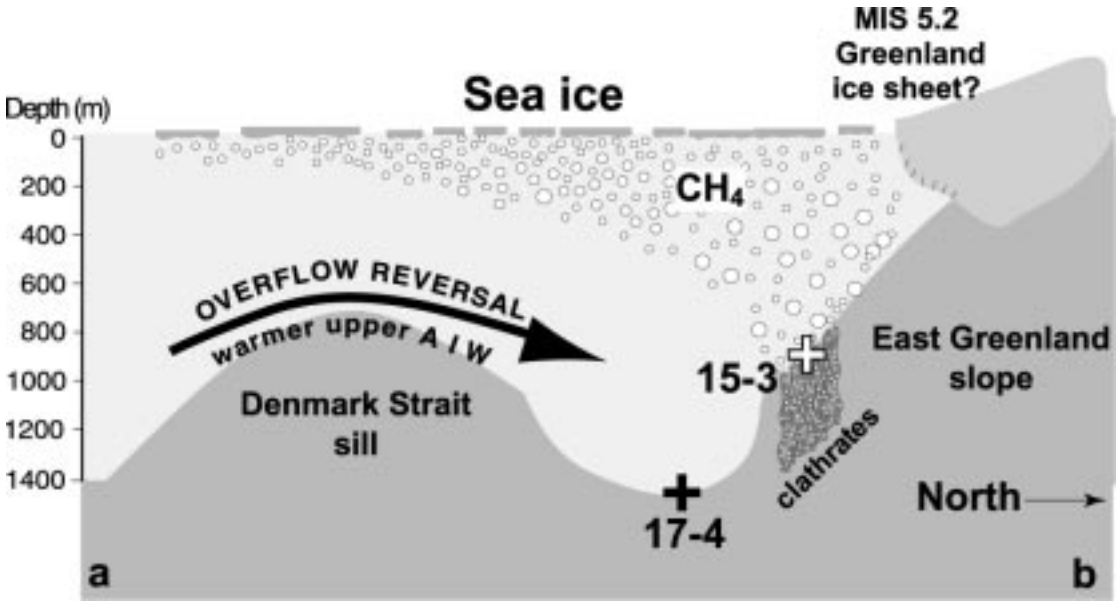

Figure 5. Paleoceanographic model profile across Blosseville Basin during periods of Denmark Strait Overflow (DSO) reversals and incursion of relatively warm Atlantic Upper Intermediate Water (AIW) (adapted from Kennett et al., 2000). Bubbles indicate CH_4 blow-out plume from East Greenland slope. MIS—marine isotope stage.

Rasmussen and Thomsen (2004) first postulated for DO stadials that AIW (from the Mediterranean Outflow) may have debouched into the Nordic Seas, below stratified cold surface water. This warming and a relative sea-level lowstand (Lambeck and Chappell, 2001) during MIS 5.2 possibly led to clathrate instability near to site 15-3 (clathrates at 700 mwd become unstable at 8 °C; Dickens and Quinby-Hunt, 1994) (Fig. 5). Although bottom simulating reflections have rarely been encountered along the Greenland slope, clathrates of pre-Quaternary origin are likely to occur (B. Larsen, 2005; personal comm.). In addition, a methane origin for the $\delta^{13}C$ excursions is supported by (1) coeval ^{13}C depletion at different sites, decreasing from the Greenland slope (Site 15-3) toward the east; and (2) isotopically light authigenic overgrowth at site 15-3, where no other source of ^{13}C-depleted organic carbon is available. Such overgrowth is common for CH_4-enriched vent regions (Eichhubl et al., 2000).

The impact of methane-influenced DIC on primary tests of *N. pachyderma* can be explained by the conceptual model that rising CH_4 bubbles reached the stratified surface water of the southward flowing EGC (Fig. 5), there producing a significant ^{13}C depletion of DIC. Moreover, extensive sea ice probably delayed the gas exchange between ocean and atmosphere, increased CH_4 concentration in surface water, and thereby prolonged the residence time of the negative $\delta^{13}C$ shift up to a

summer/growth season (2-3 months). In total, the amount of CH_4 responsible for lowering the $\delta^{13}C_{DIC}$ by –2.5‰ to –4‰, (the additional lowering towards –7‰ is ascribed to diagenetic overprint) was calculated from the water volume affected (~1,900 km^3) in both the immediate bottom water and the sea ice covered, 150 meter thick surface layer of the (western) Blosseville Basin (Fig. 5), methane $\delta^{13}C$ of –65‰ versus the background $\delta^{13}C_{DIC}$ value of 0‰, and a DIC concentration of 2.2 mmol/kg, and may amount to 2.6 – 4.3 Tg equal to 3.5 – 6.5 km^3 of CH_4 for each season affected, and up to 21 to 40 km^3 of molten clathrate for every 1000 years (with 164 m^3 of gas per m^3 of clathrate at 1 atm).

Less pronounced negative $\delta^{13}C$ anomalies in core 17-4 (central Blosseville Basin) suggest a smaller negative change in surface water $\delta^{13}C$ due to eastward dilution of the CH_4 plume, but are also linked to an apparent absence of authigenesis in both planktic and benthic foraminifera at this site (based on light microscopy).

The major $\delta^{13}C$ minima of Events 1a and II match atmospheric CH_4 maxima (Blunier and Brook, 2001) during MIS 5.2, 5.1, and 3, both in terms of amplitude and duration (Fig. 3). This may support the hypothesis that destabilization of methane hydrates has contributed to increases in atmospheric CH_4 during stadial-to-interstadial warmings (Kennett et al., 2003).

In summary, a meltwater-induced cessation of deep water convection in the Greenland Sea, northward advection of warm intermediate water, and subsequent thermal instability of clathrates appear to be the most likely explanation for the extreme $\delta^{13}C$ Events 1a-1c. No such inferred meltwater pulses are yet recorded during Event II at the transition from HE 5.2 to DO interstadial 14, and hence this aspect of the hypothesis requires explanation.

ACKNOWLEDGMENTS

We thank M. Weinelt, P.M. Grootes, J. Kennett (Santa Barbara), B. Larsen (Copenhagen), and the reviewers for highly valuable comments and advice, and the German Research Foundation (DFG) for support within the Kiel Research Unit 451.

REFERENCES CITED:

Blunier, T., and Brook, E.J., 2001, Timing of millennial-scale climate change in Antarctica and Greenland during the last glacial period: Science, v. 291, p. 109–112.

Brook, E.J., Harder, S., Severinghaus, J., and Bender, M., 1999, Atmospheric methane and millennial-scale climate change, *in* Clark, P.U., et al., eds., Mechanisms of global climate change at millennial time scales: American Geophysical Union Geophysical Monograph 112, p. 165–175.

de Garidel-Thoron, T., Beaufort, L., Bassinot, F., and Henry, P., 2004, Evidence for large methane releases to the atmosphere from deep-sea gas-hydrate dissociation during the last glacial episode: Proceedings of the National Academy of Sciences of the United States of America, v. 101, p. 9187–9192.

Dickens, G.R., and Quinby-Hunt, M.S., 1994, Methane hydrate stability in seawater: Geophysical Research Letters, v. 21, p. 2115–2118.

Eichhubl, P., Greene, H.G., Naehr, T., and Maher, N., 2000, Structural control of fluid flow: Offshore fluid seepage in the Santa Barbara Basin, California: Journal of Geochemical Exploration, v. 69–70, p. 545–549.

Grootes, P.M., and Stuiver, M., 1997, $^{18}O/^{16}O$ variability in Greenland snow and ice with 10^{-3} to 10^{5} year time resolution: Journal of Geophysical Research, v. 102, no. C12, p. 26,455–26,470.

Hill, T.M., Kennett, J.P., and Spero, H.J., 2004a, High-resolution records of methane hydrate dissociation: ODP Site 893, Santa Barbara Basin: Earth and Planetary Science Letters, v. 223, p. 127–140.

Hill, T.M., Kennett, J.P., and Valentine, D.L., 2004b, Isotopic evidence for the incorporation of methane-derived carbon into foraminifera from modern methane seeps, Hydrate Ridge, northeast Pacific: Geochimica et Cosmochimica Acta, v. 68, p. 4619–4627.

Kennett, J.P., Cannariato, K.G., Hendy, I.L., and Behl, R.J., 2000, Carbon isotopic evidence for methane hydrate instability during Quaternary interstadials: Science, v. 288, p. 128–133.

Kennett, J.P., Cannariato, K.G., Hendy, I.L., and Behl, R.J., 2003, Methane hydrates in Quaternary climate change, the Clathrate Gun Hypothesis: Washington D.C., American Geophysical Union, 216 p.

Laj, C., Kissel, C., Mazaud, A., Channell, J.E.T., and Beer, J., 2000, North Atlantic paleointensity stack since 75 ka of the Laschamp event: Royal Society of London Philosophical Transactions, ser. A, v. 358, p. 1009–1025.

Lambeck, K., and Chappell, J., 2001, Sea level change through the last glacial cycle: Science, v. 292, p. 679–686.

North Greenland Ice Core Project Members, 2004, High-resolution record of Northern Hemisphere climate extending into the last interglacial period: Nature, v. 431, p. 147–151.

Paillard, D., Labeyrie, L., and Yiou, P., 1996, Macintosh program performs time-series analysis: Eos (Transactions, American Geophysical Union), v. 77, p. 379.

Rasmussen, T.L., and Thomsen, E., 2004, The role of the North Atlantic Drift in the millennial timescale glacial climate fluctuations: Palaeogeography, Palaeoclimatology, Palaeoecology, v. 210, p. 101–116.

Rathburn, A.E., Perez, E.M., Martin, J.B., Day, S.A., Mahn, C., Gieskes, J., Ziebis, W., Williams, D., and Bahls, A., 2003, Relationships between the distribution and stable isotopic composition of living benthic foraminifera and cold methane seep

biogeochemistry in Monterey Bay, California: Geochemistry, Geophysics, Geosystems, v. 4, p. 1106.

Schlueter, M., Sauter, E.J., Schulz-Bull, D., Balzer, W., and Suess, E., 2001, Fluxes of organic carbon and biogenic silica reaching the seafloor: A comparison of high northern and southern latitudes of the Atlantic Ocean, *in* Schaefer, P., et al., eds., The northern North Atlantic: A changing environment: Berlin, Springer, p. 225–240.

Smith, L.M., Sachs, J.P., Jennings, A.E., Anderson, D.M., and de Vernal, A., 2001, Light $\delta^{13}C$ events during deglaciation of the East Greenland continental shelf attributed to methane release from gas hydrates: Geophysical Research Letters, v. 28, p. 2217–2220.

van Kreveld, S., Sarnthein, M., Erlenkeuser, H., Grootes, P., Jung, S., Nadeau, M.J., Pflaumann, U., and Voelker, A., 2000, Potential links between surging ice sheets, circulation changes, and the Dansgaard-Oeschger cycles in the Irminger Sea, 60–18 kyr: Paleoceanography, v. 15, p. 425–442.

Voelker, A.H., 1999, Zur Deutung der Dansgaard-Oeschger Ereignisse in ultra-hochauflösenden Sedimentprofilen aus dem Europäischen Nordmeer (Ph.D. thesis): Kiel, University of Kiel, 180 p.

Voelker, A.H., Sarnthein, M., Grootes, P.M., Erlenkeuser, H., Laj, C., Mazaud, A., Nadeau, M.J., and Schleicher, M., 1998, Correlation of marine ^{14}C ages from the Nordic Seas with the GISP2 isotope record: Implications for ^{14}C calibration beyond 25 ka BP: Radiocarbon, v. 40, p. 517–534.

3B. Methane-induced early diagenesis of foraminiferal tests in the southwestern Greenland Sea

CHRISTIAN MILLO, MICHAEL SARNTHEIN, HELMUT ERLENKEUSER, PIET GROOTES, AND NILS ANDERSEN

Christian Millo (cm@gpi.uni-kiel.de) and Michael Sarnthein, Department of Geology, Christian-Albrechts-Universitaet, Olshausenstrasse 40, D-24118 Kiel, Germany;

Helmut Erlenkeuser, Piet Grootes, and Nils Andersen, Leibniz-Labor for Radiometric Dating and Isotope Research, Max-Eyth-Strasse 11, D-24118 Kiel, Germany.

Accepted for publication in *Marine Micropaleontology* on 25 July 2005

Abstract

Planktic and epibenthic foraminiferal $\delta^{13}C$ records at Site PS62/015-3 (southwestern Greenland Sea) reveal a series of transient events of extreme ^{13}C depletion down to –6‰ during the period 90-40 ka. Scanning electron microscope studies of the ultrastructures of foraminiferal tests suggest that ^{13}C depleted specimens are affected by some 10-20% overgrowth by authigenic calcite contributing to the light $\delta^{13}C$ signal. Incremental-leaching experiments and census counts of pristine versus overgrowth-affected specimens show that the ^{13}C depleted foraminiferal tests incorporate a primary $\delta^{13}C$ signature most likely ranging from +1 to –1.7‰ and a post-depositional $\delta^{13}C$ signature around –17 to –19.5‰. Extremely low values of productivity and organic carbon in Late Quaternary sediments along the East Greenland margin preclude organic matter as potential source of the isotopically light carbon. In contrast, thermal instability of clathrates and subsequent aerobic oxidation of (highly ^{12}C enriched) methane in pore and ocean water provide a compelling mechanism to account for the negative $\delta^{13}C$ excursions of both primary and post-depositional carbonates. Here, pore water methane may have led to a supersaturation of ^{13}C depleted bicarbonate and precipitation of isotopically light authigenic calcite on

and in foraminiferal tests, a feature that may serve as a tracer to former sites of clathrate destabilization.

Keywords: Greenland Sea, Stable carbon isotope, Clathrates, Diagenesis, Foraminifera.

3B.1 Introduction

The stable isotope composition of foraminiferal tests is widely used in paleoceanographic studies to reconstruct the physical and chemical parameters of ambient water masses. In recent years, extremely negative anomalies were frequently identified in planktic and benthic carbon isotope records at times of abrupt global warming. These events suggest that large amounts of isotopically light carbon have been released into the ocean as result of thermally-induced clathrate dissociation, light carbon that eventually has been incorporated into the Dissolved Inorganic Carbon (DIC) pool and the skeletons of marine organisms (Wefer et al., 1994; Dickens et al., 1995; Kennett et al., 2000; Hill et al., 2004). It is a matter of ongoing debate, whether such extremely negative foraminiferal $\delta^{13}C$ values derive from the DIC composition at primary calcification and/or from subsequent authigenesis (Cannariato and Stott, 2004). To address the controversy, extensive studies were carried out by several authors with conflicting and complex conclusions.

On the one hand, trace element analyses of ^{13}C depleted benthic specimens from the Hydrate Ridge (Oregon) showed a Mg/Ca ratio of 30 to 50 mmol/mol and thus indicated a post-depositional overprint (Torres et al., 2003). On the other hand, stable isotope measurements of living (rose Bengal stained) benthic individuals from active methane seeps (Rathburn et al. 2003; Hill et al. 2004) revealed that most foraminiferal tests just reflect the primary, extremely low $\delta^{13}C_{DIC}$ signal of their habitat. Furthermore, scanning electron microscope (SEM) images coupled with stable isotope data of single planktic and benthic foraminiferal tests revealed no evidence of secondary $CaCO_3$ precipitates in ^{13}C depleted individuals (Kennett et al., 2000; de Garidel-Thoron et al., 2004; Hill et al. 2004). In contrast, Lembke et al. (pers. comm.) report authigenic carbonate overgrowth which induced severe ^{13}C depletion of foraminifera obtained from methane vents near the entrance of the Sea of Okhotsk. In summary, these findings suggest that episodic methane seepage from

marine sediments leaves a primary and /or a post-depositional imprint on foraminiferal $\delta^{13}C$.

In this study we further elaborate on extreme $\delta^{13}C$ minima recently reported by Millo et al. (in press, 2005). They showed planktic and epibenthic stable isotope records at Site PS62/015-3 (Blosseville Basin, East Greenland slope), which document during the last 90 000 years several transient events of ^{13}C depletion down to –6‰, a level unusual for the Nordic Seas. Organic matter can be largely dismissed as source of light carbon isotopes, since the organic carbon content in sediments along the East Greenland margin is low. On the other hand, these $\delta^{13}C$ minima appear to be linked to meltwater-induced reversals in the Denmark Strait Overflow and a dramatic bottom water warming in the Blosseville Basin during Dansgaard-Oeschger stadials. The bottom water warming, in turn, is considered as a trigger of thermal instability of clathrates, thus providing a compelling mechanism for the injection of isotopically light methane into both pore water and the ocean surface layer, where methane is subjected to aerobic oxidation and added to the local DIC.

At Site 15-3, the extreme $\delta^{13}C$ minima in planktic and benthic foraminifera appear to be linked to features of secondary overgrowth, that is to early diagenesis still within one and the same stratigraphic horizon. In contrast, coeval but less negative $\delta^{13}C_{DIC}$ excursions (~ -1.25‰) that are documented as aberrant in a planktic $\delta^{13}C$ record from neighbor Site PS62/ 017-4 don't appear paralleled by post-depositional alteration. These different records may thus suggest that early diagenetic overgrowth on foraminiferal specimens may concentrate to the vicinity of sites of hydrate destabilization. In this study we try to constrain both the extent of ^{13}C depletion representing a primary signal of methane in the water column and the extent of post-depositional, secondary $\delta^{13}C$ signatures due to authigenic carbonate.

3B.2 Study area and methods

Sediment core PS62/015-3 (referred to as core/Site 15-3; 67° 55.85‘ N, 25° 25.59‘ W, 980 m water depth) was retrieved from the Blosseville Basin which is located to the north of the Denmark Strait between East Greenland and Northwest Iceland with water depths reaching approximately 1500 m (Fig. 1).

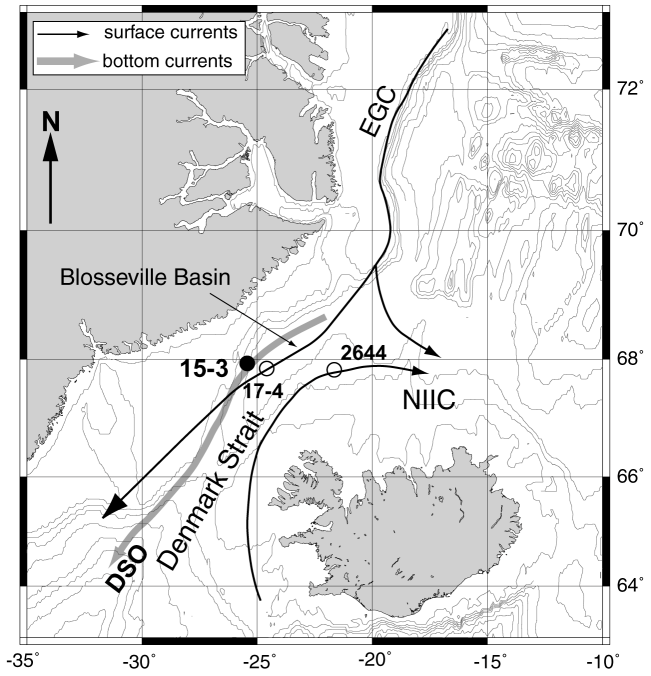

Fig. 1. Location of sites PS62/015-3 and neighbor cores PS62/017-4 and PS2644. Surface and deepwater currents in the Blosseville Basin are schematically indicated. EGC = East Greenland Current, NIIC = North Icelandic Irminger Current, DSO = Denmark Strait Overflow.

Today the area is close to an important site of deepwater formation in the central Greenland Sea and intersects the paths of the Denmark Strait Overflow and the Irminger Current. Core 15-3 is part of a core transect which includes two neighbor cores PS62/017-4 and PS 2644 farther east (Fig. 1). Analogies between both magnetic intensity and planktic $\delta^{18}O$ records of the three companion cores provided a joint chronostratigraphic framework of coeval $\delta^{13}C$ excursions in the Blosseville Basin over the last 90 000 years (details in Millo et al., in press).

Core 15-3 was sampled each 5 cm from the top down to 200 cm below sediment surface (bsf), each 2-3 cm from 200 to 400 cm bsf, and centimeter-wise down to the core bottom (636 cm). Samples were washed over a 63-µm sieve and dried at 40 °C. The concentration of foraminifera is highly variable, some core intervals being practically barren. Where possible, 25 specimens of planktic *Neogloboquadrina pachyderma* s. (Nps) (150-250 µm) and 1 to 10 specimens of epibenthic *Cibicides lobatulus* (250-400 µm) were picked for multiple and single-specimen stable isotope analysis, respectively.

Following standard preparation routines, foraminiferal samples were gently crushed, ultrasonically cleaned in ethanol, and dried. Oxygen and carbon stable isotopes were measured at the Leibniz Laboratory of Kiel University using the Kiel Carboprep line and an automated Finnigan MAT-251 mass spectrometer (analytical precision: ± 0.07‰ for $\delta^{18}O$, ± 0.05‰ for $\delta^{13}C$). $\delta^{13}C$ values of Nps were corrected for

a vital/habitat effect of +0.83‰ (Labeyrie and Duplessy, 1985) to compare with the $\delta^{13}C$ values of *C. lobatulus* that represent the $\delta^{13}C$ of DIC in ambient bottom water.

The preservation state of several hundred planktic and benthic foraminiferal tests in 130 samples was initially assessed under the binocular up to a 32 X magnification. In addition, up to 20 average individuals from 7 samples were imaged using Scanning Electron Microscopy (SEM) (Fig. 2C).

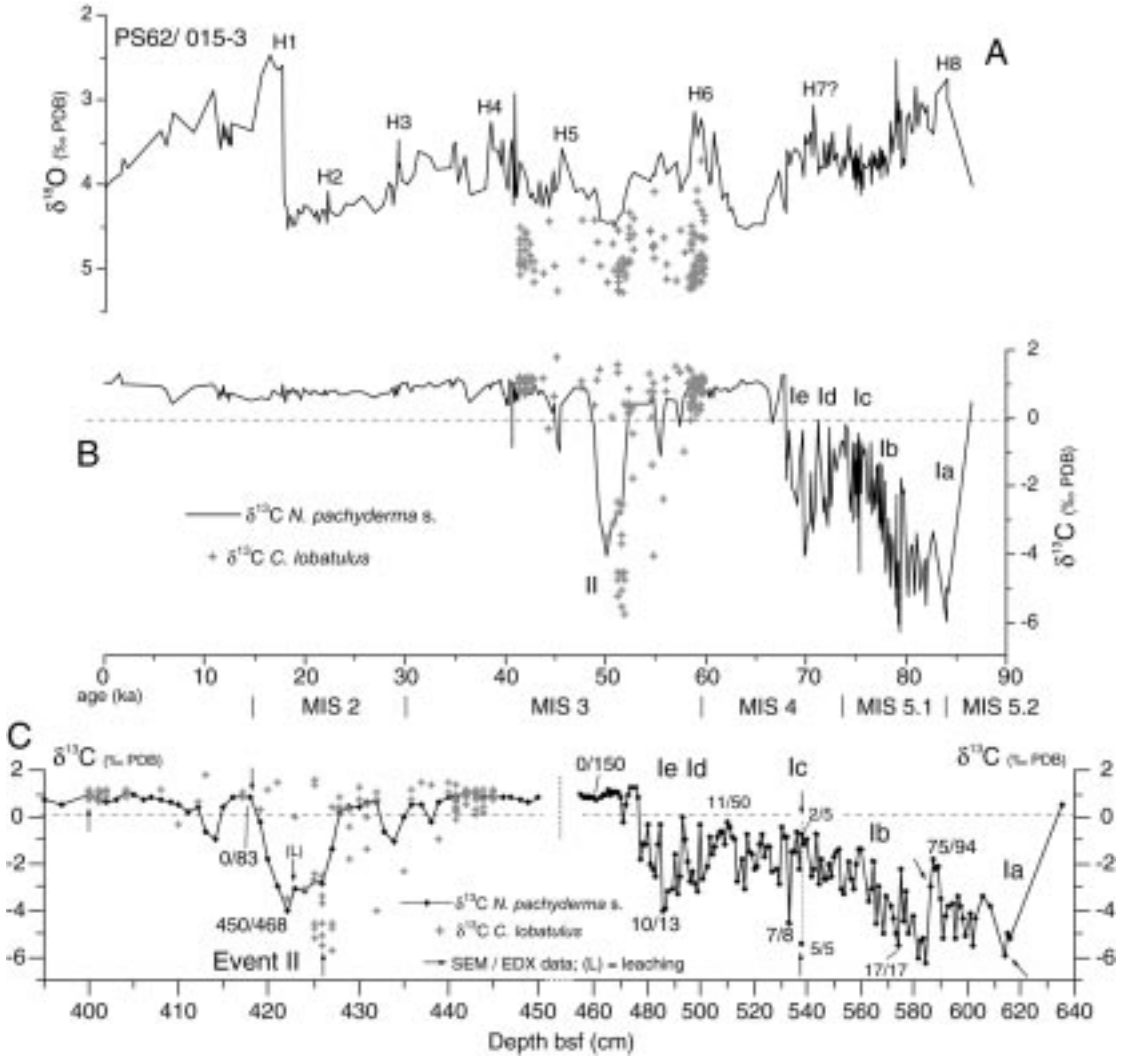

Fig. 2. (A and B): Stable-isotope records of planktic *N. pachyderma* s. (solid lines, values corrected by +0.83‰; Labeyrie and Duplessy, 1985) and epibenthic single specimens of *C. lobatulus* (+ signs) in core 15-3, plotted versus age (Millo et al., submitted). Marine Isotope Stages (MIS) and major meltwater pulses during Heinrich (H) events are numbered. Ia-e and II mark events of extreme foraminiferal ^{13}C depletion. (C): Blow-up of $\delta^{13}C$ records for Event II and Event I plotted versus core depth in cm bsf. Arrows indicate seven samples studied by SEM and EDX. Fraction numbers indicate the relative abundance of altered versus total specimens of Nps.

Foraminiferal specimens were fixed on a stub and subsequently coated with a mixture of gold and palladium to improve backscatter. Thanks to the relatively large mass of single benthic foraminifera, SEM and stable isotope analyses were carried out on separate fragments of one and the same individual. Qualitative estimates of the

trace metal content were obtained from the test surface with Energy Dispersive X-ray (EDX) (CAMSCAN Serie 2 CS 44).

To constrain more closely the primary and the secondary, diagenetic imprints on foraminiferal $\delta^{13}C$ values we also picked two subsamples of 50 Nps specimens each from a strongly ^{13}C depleted core section (423 cm bsf). These specimens were leached – in a random approach – up to 30 and 60% of the original mass using 1% HCl (0.28 mol/l). After rinsing with demineralized water, samples were cleansed in ethanol, dried, and prepared for stable isotope analysis in order to reveal potential $\delta^{13}C$ changes. Independently of the isotopic composition, the elemental composition of both the unleached and the 60–% leached shells was analyzed by EDX.

The interpretation of these experiments relied on various assumptions. (1) The proportions of primary and authigenic carbonates in foraminiferal tests were roughly constrained by visual SEM estimates to a range of 90/10 to 80/20, used as working hypothesis. For example, by studying shell fragments we compared the thickness of the overgrowth of authigenic small euhedral crystals and crystal clusters on top of pristine test walls and surfaces with the thickness of the pristine test portion itself, characterized by crystal palisades (see Fig. 3J, K and L). (2) Primary and authigenic carbonates are regarded as differentially sensitive to dissolution because of different crystal structures. (3) Accordingly, it should be possible to infer differences in the isotopic composition of both components from pre- and post-leaching $\delta^{13}C$ values and via a mass balance calculation, if the isotopic composition of the primary shell is assumed homogeneous. However, our EDX analyses show that large portions (up to 80/ 90%) of the non–dissolved shell remnants consist of non–carbonate (Table 1b) and hence are non–homogeneous.

3B.3 Results

The planktic and benthic foraminiferal $\delta^{13}C$ records of core 15-3 exhibit two major intervals of extreme ^{13}C depletion (Fig. 2; for details see Millo et al., in press). The most prominent event occurs in the older portion of the record, between 580 and 615 cm bsf (Fig. 2C), that is from 85 to 79 ka (Fig. 2B), where $\delta^{13}C$ values of Nps scatter broadly between –6.2 and –2.2‰ and subsequently increase gradually upcore to 0 and +1‰. In the lowermost portion of this Event Ia planktic foraminiferal specimens are rare, and epibenthic specimens are absent.

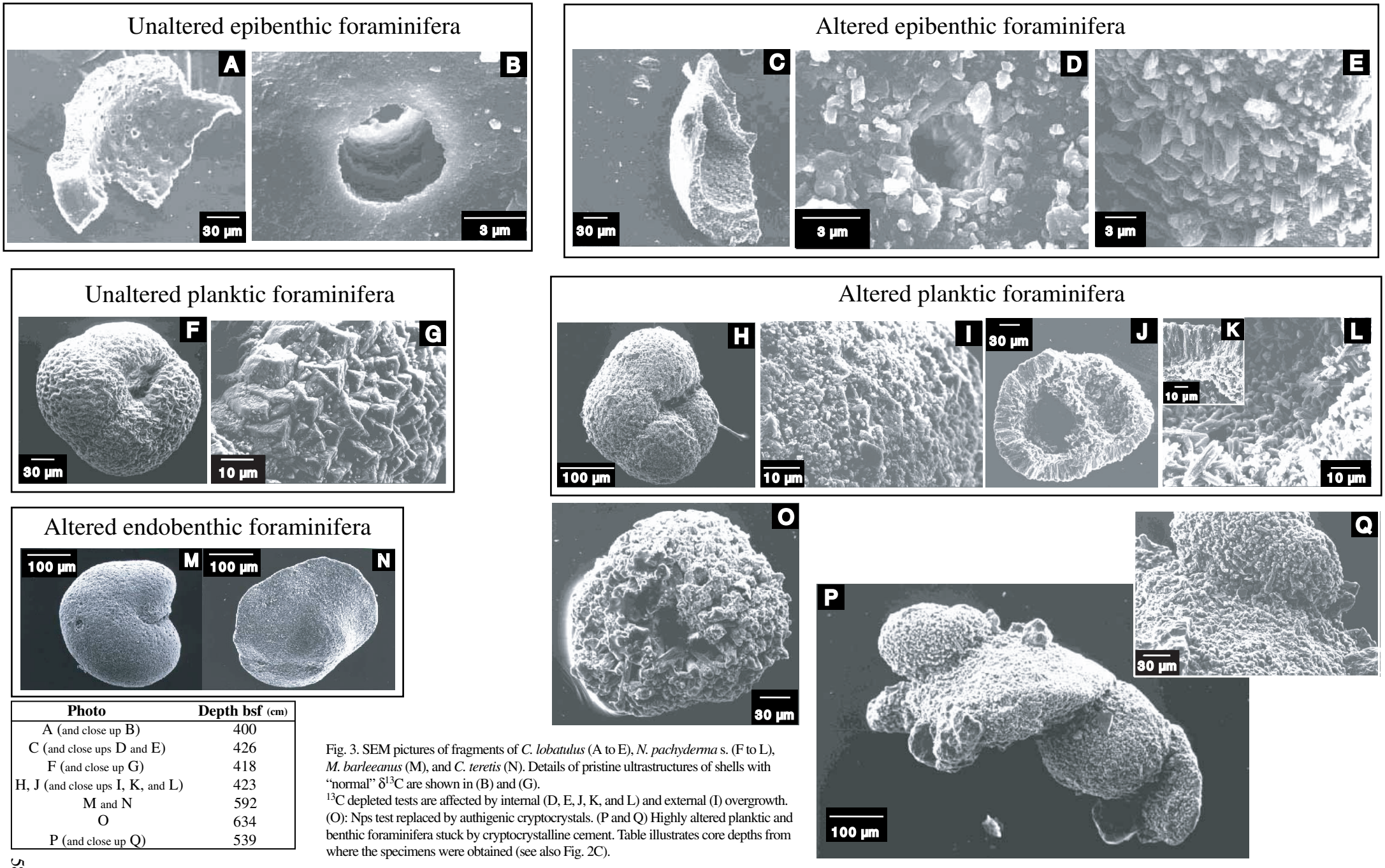

Photo	Depth bsf (cm)
A (and close up B)	400
C (and close ups D and E)	426
F (and close up G)	418
H, J (and close ups I, K, and L)	423
M and N	592
O	634
P (and close up Q)	539

Fig. 3. SEM pictures of fragments of *C. lobatulus* (A to E), *N. pachyderma* s. (F to L), *M. barleeanus* (M), and *C. teretis* (N). Details of pristine ultrastructures of shells with "normal" $\delta^{13}C$ are shown in (B) and (G). ^{13}C depleted tests are affected by internal (D, E, J, K, and L) and external (I) overgrowth. (O): Nps test replaced by authigenic cryptocrystals. (P and Q) Highly altered planktic and benthic foraminifera stuck by cryptocrystalline cement. Table illustrates core depths from where the specimens were obtained (see also Fig. 2C).

Table 1
Energy Dispersive X-ray (EDX) qualitative estimates of major trace metal contents of primary test carbonate as compared to the contents of diagenetic overgrowth in both ^{13}C depleted and non-depleted foraminiferal tests at Site 15-3. Note high Si values in leached samples.
Roman numbers in Table 1a refer to EDX-analysed specimens obtained from the same sampling interval (note that $\delta^{18}O$ values in these samples do not vary significantly).
Numbers and Greek letters in Table 1b refer to positions of EDX analyses displayed in Fig.4.
Nps $\delta^{13}C$ values are corrected for +0.83‰; (Labeyrie and Duplessy, 1985).

Depth (cm bsf)	$\delta^{18}O$ (‰ PDB)	$\delta^{13}C$ (‰ PDB)	Species		Ca (%)	Mg (%)	Al (%)	Fe (%)	Mn (%)	Si (%)
a) Unleached foraminiferal samples										
				primary test	overgrowth					
418	4.17	0.83	Nps	99.07	absent	—	—	—	—	0.93
423 (I)	4.36	-4.16	Nps	100		—	—	—	—	—
423 (I)	4.36	-4.16	Nps		91.01	4.68	—	—	—	4.31
423 (II)	4.44	-3.11	Nps	99.48		—	—	—	—	0.52
423 (II)	4.44	-3.11	Nps		83.28	3.62	—	—	9.34	3.76
423 (II)	4.44	-3.11	Nps		73.81	—	2.85	3.43	11.58	8.33
538 (I)	4.06	-0.74	Nps	92.05		1.68	1.89	—	—	4.39
538 (II)	4.06	-0.74	Nps	99.49		—	—	—	—	—
538 (III)	4.22	-5.30	Nps		81.72	3.50	1.00	2.25	7.29	4.24
586 (I)	3.58	-3.01	Nps		87.87	2.34	2.75	—	—	7.03
586 (II)	3.58	-3.01	Nps		84.39	4.60	3.36	—	—	7.66
614	2.76	-5.97	Nps		76.43	3.18	6.82	—	—	11.98
400	4.83	1.21	*C. lobatulus*	100	absent	—	—	—	—	—
426	5.00	-5.80	*C. lobatulus*		82.05	—	0.75	4.89	7.11	3.30
b) *N.pachyderma* s. after 60% leaching										
			# Fig.4:							
423 (L I)	4.41	-5.67	1	89.63		—	—	—	8.55	1.82
			2	63.36		—	—	19.11	16.20	1.33
			3	3.40		4.76	15.64	18.74	—	50.92
			4	8.32		5.88	13.69	20.49	—	44.27
			5		8.17	—	11.18	38.41	—	33.44
			6		10.23	2.98	8.31	44.45	—	24.50
			7		37.44	—	3.02	41.43	—	10.99
			8		19.19	1.69	7.07	22.91	—	43.27
423 (L II)			α	3.49		3.24	12.74	14.16	—	62.78
			β	85.43		—	0.87	10.70	—	3.00
			γ	8.55		2.33	7.43	50.09	—	24.12

A second prominent negative planktic $\delta^{13}C$ excursion occurs between 418 and 428 cm bsf (i.e. from 52 to 48 ka; Fig. 2B) reaching –4.2‰ at 422 cm (Fig. 2C; for details see Millo et al., in press). In this interval, $\delta^{13}C$ values of single epibenthic specimens exceed the planktic trend by ~ 2‰. Note that benthic $\delta^{13}C$ values at one and the same depth within the $\delta^{13}C$ excursion broadly scatter between +2 and –6‰ (Fig. 2C). Prior to and after the planktic $\delta^{13}C$ excursion $\delta^{13}C$ values of single grains of *C. lobatulus* only range between 0 and 2‰.

Under the binocular, foraminiferal tests from core depths with non-depleted $\delta^{13}C$ values appear transparent and/or whitish and, accordingly, pristine. In contrast,

core intervals corresponding to Event Ia to Ie and 2 are dominated by yellowish-brownish tests which exhibit a microgranular structure at the shell surface. Subsequent SEM studies of 7 selected samples (marked in Fig. 2C) reveal that specimens obtained from non-excursion intervals exhibit a distinct primary ultrastructure (Fig. 3 A, B, F, and G), whereas those characterized by microgranular appearance are affected by cryptocrystalline overgrowth, especially in the interior of the tests (Fig. 3 C to E, and H to N). This feature likewise affects planktic, epi-, and endobenthic species. Porous species such as Nps are more extensively altered than less porous species such as *C. lobatulus*. The overgrowth is more evident inside foraminiferal chambers where crystals (up to 10 µm long) appear euhedral and grow in clusters developing inward from the internal wall which itself appears little altered (Fig. 3 C to E, and H to L). Only in extremely altered specimens, a cryptocrystalline cement replaces almost entirely the original test (Fig. 3 O) and even may glue together altered planktic and benthic specimens (Fig. 3 P and Q).

EDX estimates of the composition of the overgrowth portion suggest that it consists of almost equal portions of $CaCO_3$ and SiO_2, enriched in Mg, Al, Fe, Mn, whereas the primary test fractions show only minor percentages of compounds other than $CaCO_3$ (Table 1). However, the concentrations of Mg possibly reveal an authigenic enrichment, but no conclusive differences for primary and secondary calcite.

Since each planktic $\delta^{13}C$ value averages the composition of 5 to 25 tests, we also roughly assessed the internal variability of $\delta^{13}C$ values by measuring separately two selected subsamples from 538 cm bsf (Event Ic), each made up by five Nps (Table 1a). Specimens that appear to be strongly overcrusted under both the binocular and SEM yielded a $\delta^{13}C$ value of –5.30‰, whereas specimens that look less affected gave a $\delta^{13}C$ value of –0.74‰ (Fig. 2C). Accordingly, different planktic $\delta^{13}C$ values also reflect the relative abundance of specimens with a different degree of secondary overgrowth.

Two planktic subsamples from 423 cm bsf (Event II) from which 30 and 60%, respectively, of the original mass was removed by leaching with 1 % HCl, show pre-leaching $\delta^{13}C$ values of –3.20 and –4.20‰. Post-leaching $\delta^{13}C$ values are slightly more negative than pre-leaching values and reach –5.70‰ after 60-% leaching (Table 2).

This experiment started from the assumption that primary and secondary calcite may have a different response to leaching. Based on visual SEM inspection (Fig. 4A to D) of Nps tests after 60-% leaching major portions of the test remnants may belong to the primary skeleton (J. Kennett; pers. comm.).

Table 2

Results of two incremental-leaching experiments of two subsamples of Nps tests (423 cm bsf).

PRE-LEACHING $\delta^{13}C$ VALUES ($\delta^{13}C_{T_1}$)	$\delta^{13}C$ VALUES AFTER 30 % LEACHING		$\delta^{13}C$ VALUES AFTER 60 % LEACHING	
	Residual tests ($\delta^{13}C_{T_2}$)	Leached portion ($\delta^{13}C_{leached}$)	Residual tests ($\delta^{13}C_{T_3}$)	Leached portion ($\delta^{13}C_{leached}$)
-3.20	-4.45	-0.20	-5.70	– -1.70
-4.20		– -3.70		-3.20

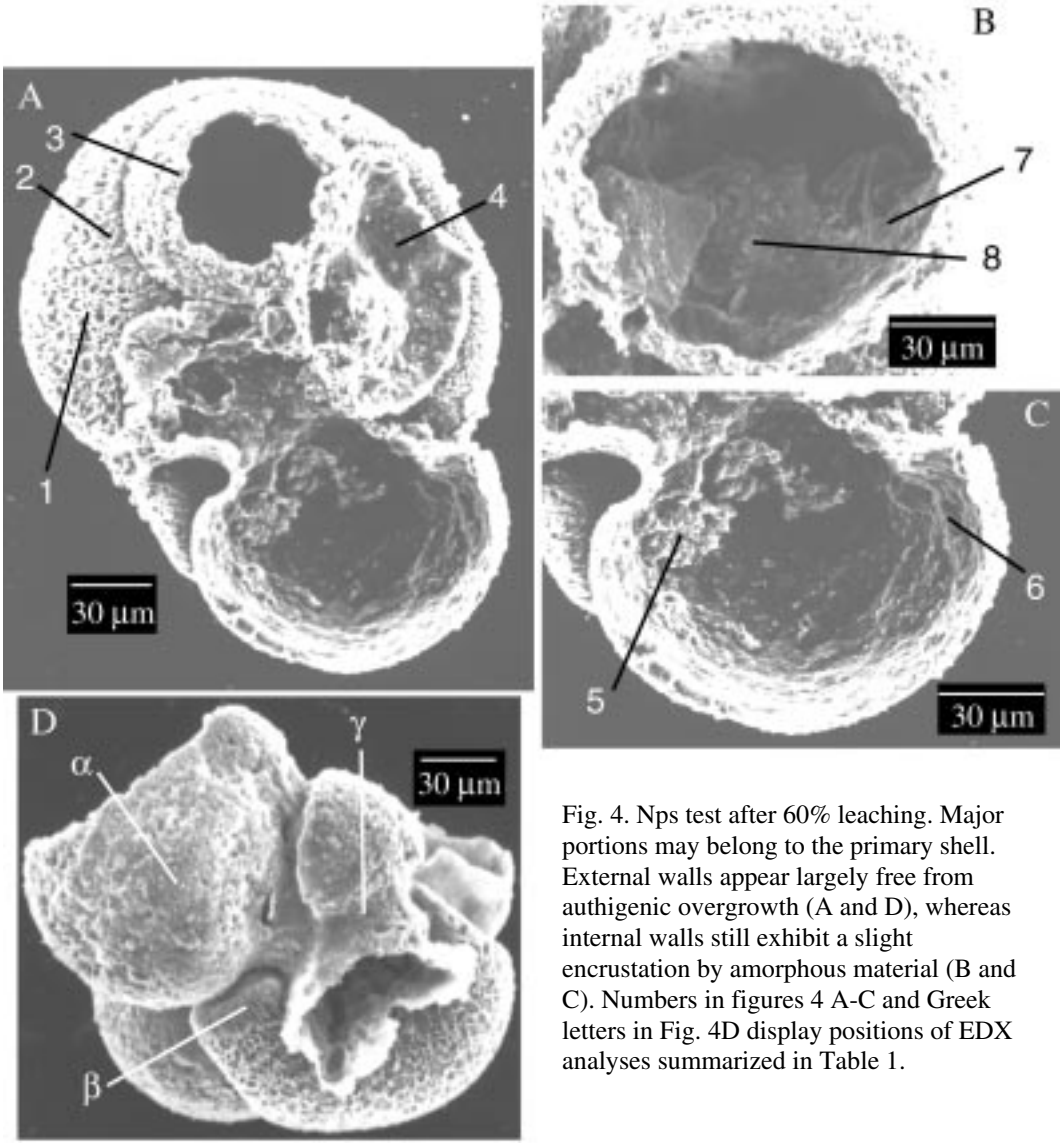

Fig. 4. Nps test after 60% leaching. Major portions may belong to the primary shell. External walls appear largely free from authigenic overgrowth (A and D), whereas internal walls still exhibit a slight encrustation by amorphous material (B and C). Numbers in figures 4 A-C and Greek letters in Fig. 4D display positions of EDX analyses summarized in Table 1.

On the other hand, these remnants mainly consist of non carbonate compounds as outlined above (Table 1b). This means that the shell carbonate has been already largely replaced by silica, although the shell remnants appear pristine after 60-%

leaching. This implies that our visual estimates of primary versus secondary shell carbonates may be misleading and that the composition of the primary shell cannot be considered as strictly homogeneous.

3B.4 Discussion

The $\delta^{13}C$ values of planktic Nps specimens affected by secondary overgrowth integrate a mixture of carbon isotope signatures formed at primary and secondary / authigenic calcification. If we assume the primary shell of Nps and the secondary calcite, respectively, are isotopically homogeneous, we can consider them as end members yielding the various isotope values observed by mixing. The results of the leaching experiments can be used to estimate via isotopic mass balance calculations the possible combinations of isotopic end member compositions and thus the possible range of isotopic compositions for primary shell and overgrowth. SEM estimates suggesting the secondary overgrowth may amount to 10 to 20% of the total tests further restrict the ranges. The calculations will give only an approximation since (1) Nps is building its test across different habitat ranges with differential stages of ventilation and DIC composition (e.g., Simstich et al., 2002) and (2) in view of the EDX estimates on strongly leached Nps remnants (Table 1b).

We use the following mass balance equation:

$$\delta^{13}C_T = P\,\delta^{13}C_P + S\,\delta^{13}C_S \qquad (1)$$

where $\delta^{13}C_T$ is the $\delta^{13}C$ value of the total Nps test; P is the percentage of the primary Nps test (supposedly amounting to 80 - 90%) with an isotopic composition $\delta^{13}C_P$, and S is the percentage of the authigenic component (20 - 10%) with an isotopic composition $\delta^{13}C_S$, and P + S = 1. Moreover, to constrain our mass balance estimates also the following numbers need to be considered: Provided 60% of the total tests with initial $\delta^{13}C_{T1}$ values of either –3.2‰ or –4.2‰ were dissolved (Fig. 5B) and the post-leaching $\delta^{13}C_{T3}$ of the remaining 40% is ~ –5.7‰, we calculate the isotopic composition of the dissolved test portions as $\delta^{13}C_{leached}$ = ~ –1.7 or –3.2‰, respectively.

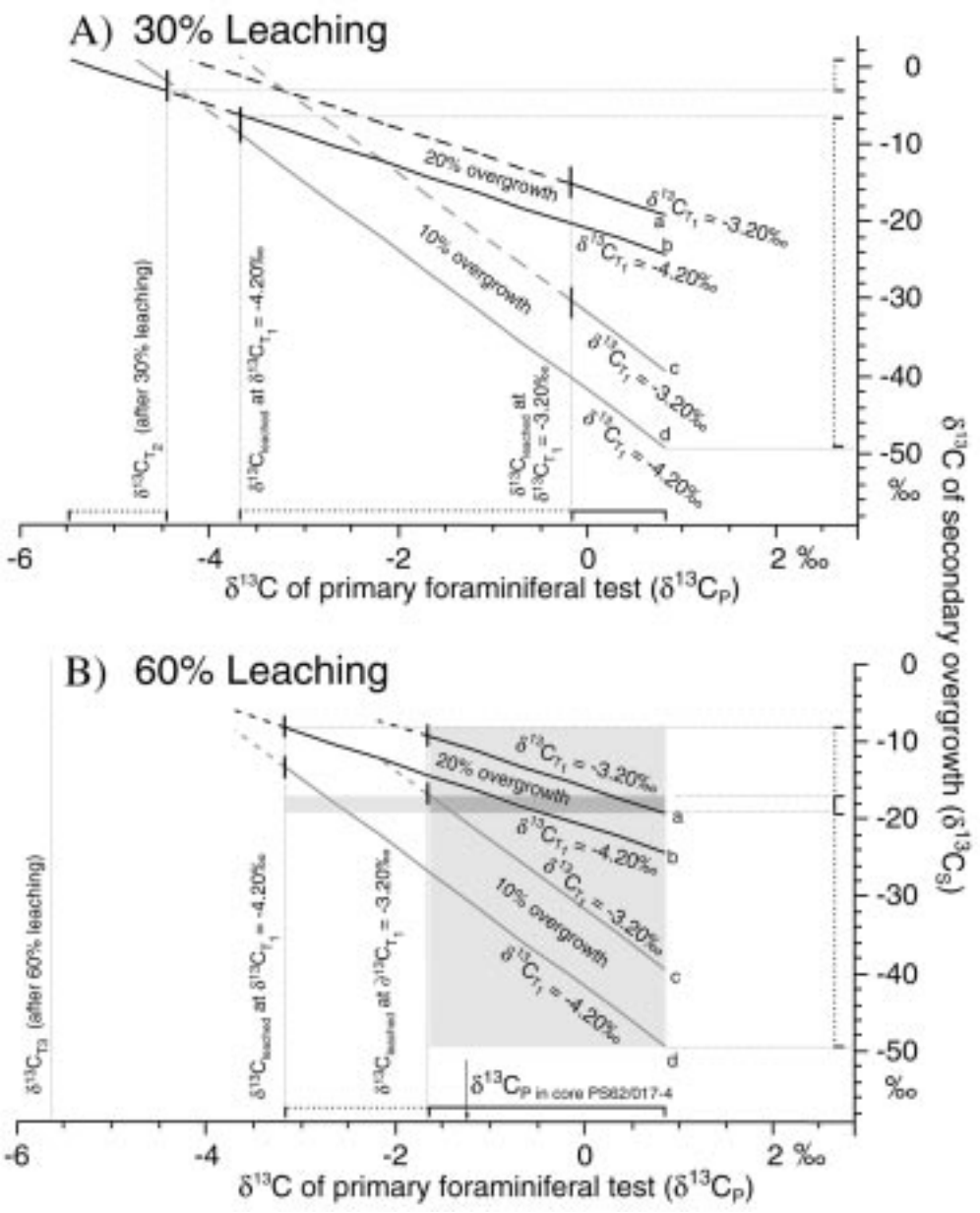

Fig. 5. Range of $\delta^{13}C$ endmembers in a supposed mixture of primary (90% or 80%) Nps tests ($\delta^{13}C_P$) and secondary (10% or 20%) overgrowth ($\delta^{13}C_S$). Endmember values were inferred from two incremental leaching experiments (A and B) evaluated by mass balance calculation and from two SEM-based estimates of the portions of primary (P) and secondary (S) calcite. $\delta^{13}C$ values are corrected by +0.83‰ (Labeyrie and Duplessy, 1985). Isolines represent pairs of endmember values that satisfy the constraints of both pre-leaching ($\delta^{13}C_{T1}$) and post-leaching $\delta^{13}C_T$ values for total tests from 423 cm bsf in core PS62/015-3. Lines **a** and **c** stand for $\delta^{13}C_{T1}$ = -3.2‰; lines **b** and **d** for $\delta^{13}C_{T1}$ = -4.2‰; $\delta^{13}C_{T2}$ and $\delta^{13}C_{T3}$ stand for the respective $\delta^{13}C$ values after 30% and 60% leaching. Dashed isolines show endmember values that do not account for post leaching $\delta^{13}C_{T2}$ (-4.45‰) and $\delta^{13}C_{T3}$ (-5.70‰) values. Solid brackets indicate overlap of solid isolines for all four experiment cases. Dashed brackets represent intervals, where only 1 to 3 isolines of the four experiments overlap. Differential degrees of likelihood for $\delta^{13}C_P$ and $\delta^{13}C_S$ endmember values are revealed by dark and light grey shadings. Arrow indicates $\delta^{13}C_P$ value (-1.25‰) of Nps in coeval $\delta^{13}C$ minimum of core PS62/017-4 plotted for comparison.

Possible combinations of $\delta^{13}C_P$ and $\delta^{13}C_S$ define lines in the $\delta^{13}C_P$ /$\delta^{13}C_S$ plot (Fig 5). These four lines calculated for two different $\delta^{13}C_{T1}$ values (Table 2) and two different amounts of overgrowth (10 %/20%) delineate the probable range of $\delta^{13}C_P$ and $\delta^{13}C_S$ values which can explain for the $\delta^{13}C_T$ values measured both prior and after the 30 % and the 60 % leaching tests as well as $\delta^{13}C_{leached}$ (Fig. 5 A and B).

Those $\delta^{13}C$ mixing ratios of $\delta^{13}C_P$ and $\delta^{13}C_S$ endmember values must be discarded (hatched lines in Fig. 5), which cannot be reconciled with the measured $\delta^{13}C_{T3}$ and/or $\delta^{13}C_{leached}$ values, that means the values that occur in the field between that of the undissolved (e.g., $\delta^{13}C_{T3}$ -5.70‰; Fig. 5B) and that of the dissolved portions (e.g., $\delta^{13}C_{leached}$ = -1.70 or –3.20‰; Fig. 5B) of Nps tests. Accordingly, one may infer from Fig. 5B that $\delta^{13}C_{T1}$ values of –3.20 to –4.20‰ correspond to a range of $\delta^{13}C_P$ values from ~ 1‰ to –3.20‰ mixed with authigenic $\delta^{13}C_S$ values ranging from -8 to -50‰.

This broad range of remaining variability was further constrained by searching for a common solution for the four cases studied in the leaching experiment. Solutions of equation (1), which result in common permil values for all four solid isolines ($\delta^{13}C_P$ = 1‰ to –1.70‰ vs. $\delta^{13}C_S$ = -17 to -19.5‰; dark-shaded band in Fig. 5B) are considered to represent the range of maximum likelihood for planktic foraminifera. Fields with common solutions for one to three solid isolines (grey shaded) are regarded to outline less likely ranges of $\delta^{13}C_P$ and $\delta^{13}C_S$. The results of the 30-% leaching experiment (Fig. 5A) led to a more disperse distribution of potential $\delta^{13}C_P$ / $\delta^{13}C_S$ endmembers. No clear ranges of maximum likelihood can be delineated.

The outlined magnitude of $\delta^{13}C_S$ occurs within the range measured at several locations on authigenic carbonate precipitates close to hydrocarbon seepage (e.g. Eichhubl et al., 2000). Likewise, the range of $\delta^{13}C$ values of primary tests is comparable with that of published planktic $\delta^{13}C$ anomalies interpreted as the result of episodes of abnormal ^{13}C depletion of DIC in the ocean surface water, caused by (local) dissociation of methane hydrate (Kennett et al., 2000; de Garidel-Thoron et al., 2004). In the then ice covered southwestern Greenland Sea thermal instability of clathrates was suggested by Millo et al. (in press) who proposed a possible link to Late Pleistocene inversions of the Denmark Strait Overflow.

The most negative spikes in planktic $\delta^{13}C_T$, named events Ia to Ie at Site 15-3, match prominent $\delta^{18}O$ minima characteristic of Heinrich events 8 and 7 (Fig. 2 A and

B). Different from the $\delta^{13}C$ minima, these $\delta^{18}O$ minima which document major meltwater pulses (Millo et al., in press), do not vary neither with the presence or absence of authigenic overgrowth nor with the intensity of shell leaching (Table 1).

According to Millo et al. (in press) high concentrations of methane can be assumed for short time intervals in the sedimentary microenvironment of the East Greenland continental margin, concentrations that may have promoted the coeval precipitation of ^{13}C depleted authigenic carbonate in epibenthic, endobenthic, and planktic foraminiferal tests at Site 15-3. This conclusion is supported by increasing percentages of altered Nps tests with decreasing values of $\delta^{13}C_T$ within narrow stratigraphic horizons, with a special increase of altered tests from –0.80‰ to –1.70‰ (Fig. 6). This trend is in harmony with the pattern in Fig. 5B, where $\delta^{13}C_P$ values of less than –1.70‰ were found to be less likely. For comparison, coeval methane affected $\delta^{13}C_T$ minima at neighbor Site 17-4 which lies distant from the Greenland margin on the floor of the Blosseville Basin (Fig. 1) are not linked to any features of secondary overgrowth and do not drop below –1.25‰. This value may thus come close to the approximate ultimate limit of ^{13}C depletion in near-surface water DIC of the then ice covered Greenland Sea.

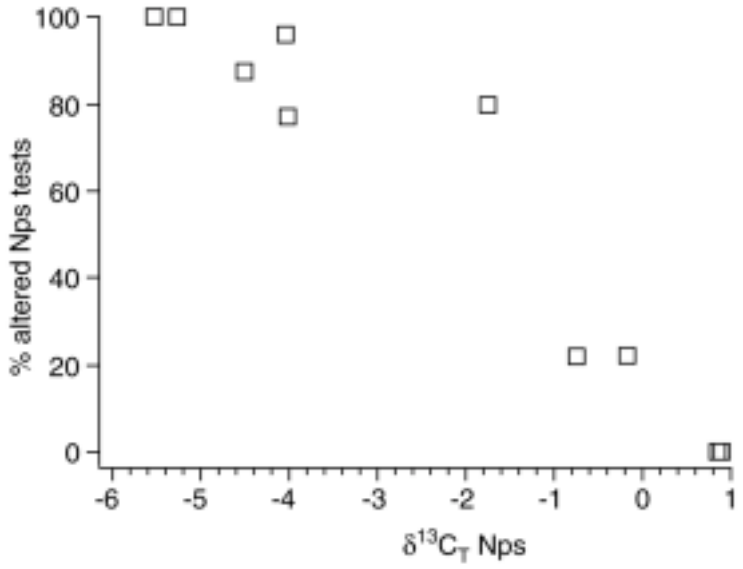

Fig. 6. Percentages of diagenetically altered Nps tests versus $\delta^{13}C_T$ values corrected for +0.83‰ (Labeyrie and Duplessy, 1985). Each $\delta^{13}C_T$ value averages the composition of 5 to 25 tests. The percentage of altered tests increases significantly below $\delta^{13}C_T$ = –1.70‰.

Examples of post-depositional ^{13}C depletion analogous to the postulated vents at Site 15-3 were observed in benthic foraminifera obtained from the active methane vent regions near the entrance on the Sea of Okhotsk (Lembke et al., pers. comm.). In our study area, alternative sources for isotopically light carbon in pore fluids such as the oxidation of organic matter can be dismissed since the organic carbon content in Late Pleistocene sediments along the East Greenland margin is extremely low (Schlueter at al., 2001; Nam et al., 1995).

We interpret the origin of the outlined short-lasting depletion of primary and authigenic $\delta^{13}C$ values in both planktic and benthic foraminiferal tests as quasi-coeval within narrowly constrained stratigraphic horizons, because also the pure primary shells associated with altered shells already show an aberrant signal of ^{13}C depletion (e.g., in sample 538 cm bsf, Fig. 2C, also Fig. 6). Accordingly, an increasing degree of early diagenesis of foraminiferal tests may possibly serve as indicator for the vicinity of core locations to sites of transient past clathrate destabilization, sites that today do not show the slightest release of methane.

3B.5 Conclusions

- Aerobic oxidation of methane in free ocean water necessarily caused a distinct $\delta^{13}C$ shift of DIC in sea water ambient to the primary calcification of foraminifera obtained from well confined stratigraphic horizons in core 15-3 from the East Greenland continental slope (Millo et al., in press). On top of this shift, pore water methane led to a supersaturation of ^{13}C depleted bicarbonate and the precipitation of ^{13}C depleted secondary carbonate on and in foraminiferal tests.
- Visual SEM-based estimates for ^{13}C depleted foraminiferal tests led to the working hypothesis that these shells consist of a mixture of primary calcite and authigenic carbonate overgrowth with relative proportions of 80-90 versus 10-20%.
- EDX-based analyses that focused on the element composition of both primary and authigenic shell portions show that the authigenic fraction is enriched in silica, iron, and manganese. After leaching 60% of two planktic foraminiferal samples, both the primary and secondary portions in shell remnants of two

randomly selected Nps specimens consist of non–carbonate elements that amount to 60 to 95%, thus suggesting a major replacement of $CaCO_3$.

- Both leaching experiments (dissolving 30 and 60 % of the original shell mass, respectively) and census counts of pristine vs. overgrowth-affected foraminiferal tests helped to constrain more closely the carbon isotope composition of primary and authigenic portions of foraminifera. The results suggest that planktic foraminiferal tests from methane-induced ^{13}C depleted horizons integrate a primary $\delta^{13}C$ signature most likely ranging from 1 to –1.70‰ and a diagenetic $\delta^{13}C$ signal around –17 to –19.5‰.
- If our conclusions are correct, in particular, if the finding is correct that the secondary overgrowth formed only shortly after the deposition of the already ^{13}C depleted primary tests, the increase in overgrowth of light authigenic carbonate on top of primary ^{12}C enriched foraminiferal tests may serve as tracer to constrain former sites of clathrate destabilization.

Acknowledgments

We are grateful to J.P. Kennett (S. Barbara CA), L. Lembke, T. Hill, M. Weinelt, and an anonymous reviewer for valuable comments and advice. We acknowledge U. Schuldt and various students for assisting with SEM exposures. This study was supported by the German Science foundation within Research Theme FOR 451.

References

Cannariato, K.G., Stott, L.D., 2004. Evidence against clathrate-derived methane release to Santa Barbara Basin surface waters? Geochemistry Geophysics Geosystems 5 (5), doi. 10.1029/2003GC000600.

de Garidel-Thoron, T., Beaufort, L., Bassinot, F., Henry, P., 2004. Evidence for large methane releases to the atmosphere from deep-sea gas hydrate dissociation during the last glacial episode. PNAS 101, 9187-9192.

Dickens, G.R., O'Neil, J.R., Rea, D.K., Owen, R.M., 1995. Dissociation of oceanic methane hydrate as a cause of carbon isotope excursion at the end of the Paleocene. Paleoceanography 10, 965-971.

Eichhubl, P., Greene, H.G., Naehr, T., Maher, N., 2000. Structural control of fluid flow: offshore fluid seepage in the Santa Barbara Basin, California. Journal of Geochemical Exploration 69-70, 545-549.

Hill, T.M., Kennett, J.P., Spero, H.J., 2004. High-resolution records of methane hydrate dissociation: ODP Site 893, Santa Barbara Basin. Earth & Planetary Science Letters 223, 127-140.

Kennett, J.P., Cannariato, K.G., Hendy, I.L., Behl, R.J., 2000. Carbon isotopic evidence for methane hydrate instability during Quaternary interstadials. Science 288, 128-133.

Labeyrie, L.D., Duplessy, J.C., 1985. Changes in the oceanic $^{13}C/^{12}C$ ratio during the last 140 000 years: High–latitude surface water records. Palaeogeography, Palaeoclimatology, Palaeoecology 50, 217-240.

Millo, C., Sarnthein, M., Erlenkeuser, H., Frederichs, T., 2005. Methane-driven Late Pleistocene $\delta^{13}C$ minima and overflow reversals in the S.W. Greenland Sea. Geology 33, 4 pp. (in press).

Nam, S-I., Stein, R., Grobe, H., Hubberten, H., 1995. Late Quaternary glacial-interglacial changes in sediment composition at the East Greenland continental margin and their paleoceanographic implications. Marine Geology 122, 243-262.

Rathburn, A.E., Perez, E.M., Martin, J.B, Day, S.A., Mahn, C., Gieskes, J., Ziebis, W., Williams, D., Bahls, A., 2003. Relationships between the distribution and stable isotopic composition of living benthic foraminifera and cold methane seep biogeochemistry in Monterey Bay, California. Geochemistry Geophysics Geosystems 4, p. 28.

Schlueter, M., Sauter, E.J., Schulz-Bull, D., Balzer, W., Suess, E., 2001. Fluxes of organic carbon and biogenic silica reaching the seafloor: A comparison of high northern and southern latitudes of the Atlantic Ocean. In: Schaefer, P. et al., (Eds.), The Northern North Atlantic: A changing environment. Springer, Berlin, pp. 225-240.

Simstich, J., Sarnthein, M., Erlenkeuser, H., 2002. Paired $\delta^{18}O$ signals of *N. pachyderma* (s) and *T. quinqueloba* show thermal stratification structure in Nordic Seas. Marine Micropaleontology 912, 1-19.

Torres, M.E., Mix, A.C., Kinports, K., Haley, B., Klinkhammer, G.P., McManus, J., de Angelis, M.A., 2003. Is methane venting at the seafloor recorded by $\delta^{13}C$ of benthic foraminifera shells? Paleoceanography 18 (3) 1062, doi: 10.1029/2002PA000824.

Wefer, G., Heinze, P.M., Berger, W.H., 1994. Clues to ancient methane release. Nature 369, p. 282.

General Acknowledgments

I wish to thank Prof. Michael Sarnthein for the continuous supervision of my study and for his scientific input and advice.

I am thankful to Dr. Mara Weinelt, who kindly supported me with her expertise in micropaleontology and for her patient explanations, especially with regard to reconstructions of ocean water density.

I owe my gratitude to Prof. Pieter M. Grootes for his important contribution to this study and for numerous discussions and valuable suggestions. I also thank a lot his team for the quality of AMS- ^{14}C datings.

A special thank to Prof. James Kennett for his fundamental scientific support, in particular with regard to the interpretation of extreme primary and post-depositional foraminiferal ^{13}C-depletions.

I am particularly thankful to Dr. Helmut Erlenkeuser, who took care of several hundred stable-isotope analyses, for his scientific advice and for long, interesting discussions about physical processes involving stable isotopes and sample preparation procedures.

I thank Dr. Nils Andersen for carrying out leaching experiments on foraminiferal tests and for most fruitful exchange of ideas.

I am greatly indebted to Karin Kissling, Claudia Sieler, Dörte Gudehus, Nadine Gehre, and Wolfgang Reimers for their kindness and technical assistance. I also thank Ute Schuldt and his team for SEM exposures.

I wish to express my sincere and profound gratitude to several students, who took care of preparation of several hundred samples with accuracy and punctuality. They are Pina Springer, Diana Magens, Dorothee Petereit, Antje Klug, Rena Isemer, and Marina Remetin.